Aged and obscured wildfire smoke associated with downwind health risks

Taekyu Joo[1,2], Mitchell J. Rogers[1], Catelynn Soong[1], Tori Hass-Mitchell[1], Seulkee Heo[3], Michelle L. Bell[3], Nga L. Ng[4,5,6], *Drew R. Gentner[1]

[1]Department of Chemical and Environmental Engineering, Yale University, New Haven, CT, USA
[2]Department of Earth and Environmental Sciences, Korea University, Seoul, South Korea
[3]School of the Environment, Yale University, New Haven, CT, USA
[4]School of Chemical and Biomolecular Engineering, Georgia Institute of Technology, Atlanta, GA, USA
[5]School of Earth and Atmospheric Sciences, Georgia Institute of Technology, Atlanta, GA, USA
[6]School of Civil and Environmental Engineering, Georgia Institute of Technology, Atlanta, GA, USA

*Corresponding author: Drew R. Gentner (drew.gentner@yale.edu)

Abstract

Fine-mode particulate matter ($PM_{2.5}$) is a highly detrimental air pollutant produced in large quantities from wildfires, which are increasing with climate change. Leveraging advanced chemical measurements in conjunction with source apportionment and health risk assessments, we quantified the stark pollution enhancements during Canadian wildfire smoke transport to New York City at its peak over June 6-9, 2023. Interestingly, we also observed lower-intensity, but frequent, multi-day wildfire smoke episodes during May-June 2023, which risk exposure misclassification as generic aged organic $PM_{2.5}$ given its extensive chemical transformations during 1-6+ days of transport. This smoke-related organic $PM_{2.5}$ showed significant associations with asthma exacerbations, and estimates of in-lung oxidative stress demonstrate the health risks of increasingly-frequent smoke episodes and potential enhancements with chemical aging. Avoiding underestimated contributions of aged biomass burning $PM_{2.5}$, especially outside of peak pollution episodes, necessitates real-time chemically-resolved monitoring to enable next-generation health studies, models, and policy under far-reaching wildfire impacts.

Introduction

Air quality has substantially improved in cities and other downwind areas across the U.S. over 50+ years of policies targeting anthropogenic sources (Parrish et al., 2011). Among air pollutants, fine particulate matter ($PM_{2.5}$) has the largest effects on premature mortality (Murray et al., 2020) with contributions from both direct emissions and secondary production following the oxidation of gas- and particle-phase precursors (Palm et al., 2020). Given its health effects, the U.S. $PM_{2.5}$ annual standard was recently lowered to 9 μg m^{-3} but remains above the World Health Organization guideline of 5 μg m^{-3}. Simultaneously, due to climate change, wildfires have emerged as increasingly important sources of $PM_{2.5}$ as well as other air pollutants and reactive compounds (Burke et al., 2023; Bourgeois et al., 2021). The composition of wildfire and other biomass burning smoke has been increasingly investigated, including laboratory combustion experiments (Koss et al., 2018; Hatch et al., 2015), oxidation chamber studies (Coggon et al., 2019; Lim et al., 2019; Joo et al., 2019; Joo et al., 2024), and aircraft-based measurements of

emissions and their downwind evolution (Xu et al., 2022; Hayden et al., 2022; Jolleys et al., 2012; Permar et al., 2021), using techniques spanning from bulk characterization of chemical and physical properties to detailed chemical speciation (Hodshire et al., 2019b; Liang et al., 2022; Palm et al., 2020).

Wildfires have increased in intensity and burned acreage over the past four decades, with projected climate scenarios heightening the risk of more frequent and larger scale fires (Abatzoglou and Williams, 2016; Burke et al., 2023). The impacts of biomass burning events, such as wildfires, are more often exerting continental influence, with evident, but uncertain, public health risks (Rogers et al., 2020; Wu et al., 2018; O'dell et al., 2021). The June 6-9, 2023 wildfire transport event brought record-setting $PM_{2.5}$ levels to New York City (NYC), the largest and most densely populated city in the U.S., with evident visual effects on air quality. However, the stark nature of this event overshadowed other more frequent, though less dramatic, wildfire smoke effects.

To better understand the extent of wildfire smoke transport and its impact on public health, we use chemically-detailed real-time data on PM composition to examine a series of five wildfire smoke events that influenced air quality in the Eastern U.S. during May-June 2023. This includes advancing source apportionment using a combination of speciated PM data from multiple instruments to better identify and quantify the impacts of such events and avoid exposure misclassification. We then evaluate key metrics of PM composition that may modify its health effects, while also comparing the results of our chemical analysis to asthma-related hospital admissions rates across the study period to inform critical avenues of inquiry at the intersection of atmospheric chemistry and public health science.

Results

Observations and analysis of far downwind wildfire smoke in New York City

Using in-situ $PM_{2.5}$ chemical composition data from the newly installed ASCENT (Atmospheric Science and Chemistry mEasurement NeTwork) site in Queens, NY (40.74N, 73.82W, 16m above sea level), we examined five different major smoke transport events of varying intensity and chemical composition during May 15 to June 13, 2023. PM analysis occurred in real-time with 3-60 min resolution measurements of organic and inorganic aerosol components via mass spectrometry and spectroscopy, metals via energy dispersive X-ray fluorescence, and aerosol sizing via scanning particle mobility, as well as complimentary gas-phase pollutant and meteorological measurements (see Methods). The identity, origin, and impacts of the five events were examined using these new multi-instrument measurements and further supported by meteorological modeling and satellite imagery. Key statistical analyses included source apportionment via positive matrix factorization of aerosol mass spectrometry data while leveraging online metals data, as well as black/brown carbon data, to quantify the chemically-speciated contributions of transported smoke—enabling component-specific comparisons to regional health data and potential oxidative stress enhancements due to each event.

June 6-9, 2023 smoke transport from the Quebec wildfire

Smoke transport from the Quebec wildfire was greatest during June 6-9, 2023, with stark regional changes in visibility extending well beyond the metro NYC area with record-setting, reported peak $PM_{2.5}$ concentrations exceeding 24-hr EPA standards in NYC (Fig. 1a, b)—even approaching the prior wildfire-induced daily averaged $PM_{2.5}$ levels in major California cities over the 21st century (e.g., San Diego, San Francisco; Fig. S1). This 3-day concentrated plume led to increased levels of many, but not all air pollutants, including 2000%, 1140%, 686%, and 511% increases in average organic aerosols, black carbon, formaldehyde, and total metal concentrations, respectively (Fig. 1a, c; Table S1). The $PM_{2.5}$ in the plume was predominantly comprised of organic aerosols with varying enhancements in non-carbonaceous inorganic aerosol components (215%-2240%; Fig. 1c; Table S1) with a pronounced bimodal particle diameter distribution (Fig. 1d), including sizes that enable deep lung penetration (Hinds, 1999).

Capturing the broader influence of aged wildfire smoke

While the June 6-9 smoke transport event brought the most striking deterioration in air quality, our high temporal resolution observations show that there were several other pollution episodes attributed to smoke transport over the study period with average $PM_{2.5}$ concentrations ranging 7.9-20 μg m^{-3} (Fig. 1a and 2a). The location of these wildfires spanned from Northwestern Canada to Quebec with average transport times (i.e., ages) ranging 2-4 days (Fig. S2, S4 and Table S2).

As urban air is influenced by a complex mix of sources and chemical processes, accurately estimating the contribution of biomass burning to urban pollution presents a challenge but is critical for air quality research and policy to protect public health. Source apportionment analysis via positive matrix factorization of aerosol mass spectrometry data is frequently used to quantify contributions from organic aerosol source types (e.g., cooking, biomass burning, hydrocarbon combustion-related) based on their distinct mass spectral features and temporal trends (Fig. S5) (Joo et al., 2021; Jimenez et al., 2009; Ng et al., 2010; Hass-Mitchell et al., 2024).

However, in this study, outside of the major Quebec smoke transport episode, aerosol mass spectrometry alone loses its ability to identify the extent of wildfire smoke after long-distance oxidative aging diminishes the characteristic spectral peaks of biomass burning organic aerosols (i.e., *m/z* 60 and 73, mass fragments of levoglucosan) (Hodshire et al., 2019b) and renders biomass burning organic aerosols less distinguishable from other oxygenated organic aerosols with elevated signal at *m/z* 44 (Fig. S6) (Cubison et al., 2011; Vasilakopoulou et al., 2023). The air quality impacts of smoke transport to NYC were observed across four organic aerosol types (two less-oxidized biomass burning organic aerosol types and two oxygenated organic aerosol types in Fig. 2a, b), with the majority of the $PM_{2.5}$ enhancements (109-560%) appearing as generic oxidized organic aerosols. Enhancements in less-oxidized and more-oxidized oxygenated organic aerosols ranged 160-237% and 112-592%, respectively, across the four relatively smaller smoke transport events, with their chemical composition varying with plume age (Fig. 2a and Table S3). For example, over June 6-9, the main plume consisted of 46% "typical" biomass burning-related organic aerosols. Then, several days later, meteorological conditions brought more aged Quebec wildfire smoke from over the Atlantic Ocean (Fig. S2) with a greater extent of aged biomass burning-related organic aerosols and more generic oxidized organic aerosols (Fig. 2). Furthermore,

a comparison of the smoke events studied here demonstrates that the smoke episodes which were more dilute during transit (i.e., 1st-3rd events) had a greater extent of oxidation despite having a similar range of transport times as the less oxidized 5th event (Figs. 2a and Fig. S4). This is consistent with prior work showing the rate of wildfire plume photochemical aging can accelerate as the plumes continue to dilute during transportation, enhancing exposure to atmospheric radicals (Xu et al., 2022), and diminishing semivolatile biomass burning tracers in organic aerosols (Cubison et al., 2011).

Due to the photochemically-aged features of the smoke reaching NYC, our real-time trace metal measurements were key to identifying and constraining wildfire influences, especially for low-intensity or long-range transported aged smoke episodes (Vasilakopoulou et al., 2023). Potassium is often one of the most abundant metals in biomass burning aerosol emissions (Reid et al., 2005), and it has been used to ascribe $PM_{2.5}$ enhancements to wildfire smoke (Andreae, 1983; Li et al., 2003; Vasilakopoulou et al., 2023). In this study, we specifically estimated the non-dust potassium associated with smoke transport via linear regression of potassium with other mineral dust species (Ca, Fe, Ti, Cu, Ba) during background periods to quantify the fraction of potassium from other sources (i.e., mineral dust) and resolve wildfire-associated potassium with greater certainty, similar to the approach by Pachon et al. (2013) (see Methods for the detailed estimation). Elemental ratios of dust established in past literature were used to validate the calculated site-specific ratios used for dust corrections (Liu et al., 2022).

This non-dust potassium exhibited the strongest correlations with smoke-related organic aerosols ($r=0.98$) (Fig. 2c) compared to other biomass burning-related pollutants (e.g., black carbon, CO and NO_x in Fig. S7) and demonstrated consistent enhancements during periods where air mass trajectories confirmed wildfire influences. While other pollutants are also associated with wildfire smoke, the results of this study exemplify dust-corrected potassium's pronounced utility as a reliable indicator of transported smoke across diverse spatial scales, combustion conditions, and age. This is not only due to the loss of key biomass burning organic aerosol mass spectral features with aging, but also as black/brown carbon, CO, or NO_x can be outweighed by larger contributions from other urban sources or incur losses due to photobleaching (i.e., for brown carbon), which varies with plume age (Hems et al., 2021).

The composition of wildfire emissions has been shown to vary with fuel type, combustion efficiency (e.g., smoldering vs flaming), pyrolysis temperature, fire size, and interactions with background aerosol conditions (Hecobian et al., 2011; Sekimoto et al., 2018; Hodshire et al., 2019a; Jen et al., 2019). Yet, non-dust potassium captures contributions from fresh biomass burning-related organic aerosols through highly-oxidized biomass burning organic aerosols, exhibiting stronger correlations ($r \geq 0.82$) compared to the other biomass burning-relevant pollutants (Fig. S7) with an overall slope of 83.1 ± 0.7 μg μgK^{-1} and ratios with a 2σ range of 63.5-253.3 μg μgK^{-1} (Fig. 2c). Thus, real-time metals data provide powerful opportunities to identify, validate, and quantify less evident biomass burning transport events in tandem with aerosol mass spectrometry data. Nevertheless, we note that potassium also has other sources (e.g., mineral dust, coal combustion) that should be considered when using it to quantify wildfire influence. Other elements characteristic of biomass burning emissions (e.g., S, Cl, Mn, Zn, Br) were also enhanced during wildfire events here and were well-correlated with potassium during the June 6-9, 2023 event, providing additional points of confirmation (Fig. 1c and Table S4).

Downwind health risks of dilute and aged wildfire smoke

Over the wide range of 1-6+ days of oxidative aging during transport (Fig. S4 and Table S2), the organic aerosols underwent considerable transformations (Fig. 2 and Fig. S6), which can have important implications for understanding its health risks. First, the depletion of the molecular signatures of biomass burning organic aerosols outside of the major Quebec fire plume (i.e., June 6-9) poses the risk of exposure misclassification of far downwind smoke as generic oxidized organic aerosols without valuable non-reactive covariate data to confirm its contributions, specifically non-dust potassium.

Epidemiological analysis using chemically-speciated aerosol data for the May 15 - June 13, 2023 study period with repeated wildfire smoke transport events identified statistically-significant associations between daily emergency department (ED) visits for asthma and concentrations of all smoke-related organic aerosols, and also with non-dust potassium (Fig. 3a and Table S5). For example, an interquartile increase in non-dust potassium was associated with a 2.23% increase in risk of asthma ED visits (95% CI: 0.40%-4.08%). While prior analyses have observed effects when looking at the major smoke event (i.e., June 6-8) with $PM_{2.5}$ alone (Table S6) (Chen et al., 2023; Mcardle et al., 2023; Meek et al., 2023; Thurston et al., 2023), in Fig. 3a, we now show associated health effects specifically with the mix of smoke-related organic aerosols (i.e., sum of 4 factors; Fig. 2a) as well as non-dust potassium as a well-correlated independent marker of wildfire smoke (Fig. 2c), regardless of plume age. Moreover, the sum of smoke-associated organic aerosols contributions had greater health effects estimate than fresh biomass-burning organic aerosols alone (i.e., BBOA factor; Table S5).

Second, while overall $PM_{2.5}$ mass concentrations remain an important metric for evaluating health risks, multiple laboratory and epidemiological studies have presented growing evidence for the greater health effects of secondary organic aerosols compared to other aerosol components (e.g., $(NH_4)_2SO_4$, NH_4NO_3, primary organic aerosols). This includes cardiovascular risks for premature mortality (Pye et al., 2021) and enhanced potential oxidative stress of secondary organic aerosols observed via cellular and acellular assays (Liu et al., 2023; Daellenbach et al., 2020; Zhou et al., 2019; Tuet et al., 2017; Yu et al., 2022; Verma et al., 2015). There is also clear evidence for increased potential oxidative stress from more-aged, oxidized aerosols with greater reactive oxygen species (ROS) production in the respiratory track (Liu et al., 2023). Across the five major smoke transport episodes studied here, our Monte Carlo analysis consistently showed pronounced increases in potential oxidative stress of 124-1631% (median enhancements) with variations constrained using available literature data while considering uncertainties (Fig. 3b and Fig. S8). This enhancement in potential oxidative stress was recently confirmed by Vasilakopoulou et al. (2023) who observed 470-3730% enhancements in dithiothreitol (DTT) assays relative to urban background sites, concurrent with downwind wildfire-associated enhancements in aged oxygenated organic aerosols and potassium in Europe. Furthermore, while the smoke plumes transported to NYC often lost their molecular signatures (Fig. 2), the more-aged particulate matter presents a greater potential oxidative stress per unit mass on average (Fig. 3b, right axis), which could be further exacerbated by coincident wildfire- and dust-related enhancements of redox-active metals (i.e., Mn, Fe, Cu) across the smoke transport events (Table S4) (Liu et al., 2023; Lakey et al., 2016; Verma et al., 2015).

Discussion

Increased wildfire activity and its emissions are anticipated to worsen air quality thereby impacting human health over the coming decades under a changing climate. However, its effects on human health remain uncertain and potentially underestimated, which is further complicated by downwind oxidation and potential exposure misclassification of less-evident smoke-related aerosol enhancements. The acute effects of the smoke were observed in epidemiological associations (Fig. 3a). Yet, the chronic effects of increasingly frequent low-level exposures to more-aged, dilute smoke represent a major potential concern and a clear priority for future research given the enhanced potential for oxidative stress with highly-aged smoke (Fig. 3b) and repeated exposures, even far downwind.

There are multiple areas where cross-disciplinary research linking atmospheric sciences and public health communities is necessary to address pressing issues. This includes accurately categorizing the pollutant contributions, especially $PM_{2.5}$, from wildfires relative to other sources to empower next-generation epidemiological studies that advance our understanding of source-specific and speciated PM-specific health effects.

With a greater fraction of future $PM_{2.5}$ likely attributed to wildfires (and intentional biomass burning such as prescribed fires) and multi-day oxidation depleting biomass burning-related organic aerosols of key identifying mass spectral features, the $PM_{2.5}$ source apportionment strategies employed here to identify the extent of oxidation and use non-dust potassium as a confirmational analysis are key to avoid undercounting biomass burning contributions across the continuum of plume ages—both of which can be used in epidemiological studies (e.g., Fig. 3a). Thus, future studies across broader spatial scales, necessitate real-time metals measurements with corrections for other source types (e.g., dust) to effectively attribute low-level wildfire influences that appear as generic aged aerosols. Such measurements will also facilitate model validation to accurately attribute biomass burning influences, especially its likely increasing contributions to background aerosol levels, (Vasilakopoulou et al., 2023) which are increasingly important to accurately constrain with recent revisions to the $PM_{2.5}$ annual U.S. standard.

Currently, PM is the only air pollutant worldwide regulated without regard to chemical form. Epidemiological research clearly demonstrates that the chemical composition of PM impacts its risk to human health (Masselot et al., 2022). However, the characteristics of particles that are most harmful are not well established, though secondary, more-oxidized organic aerosols present likely exacerbating factors (Pye et al., 2021; Liu et al., 2023; Tuet et al., 2017). Moreover, the existing regulatory monitoring network typically used in epidemiological studies, which primarily measures $PM_{2.5}$ total mass—with many $PM_{2.5}$ components measured only via filters at approximately weekly or semi-weekly sampling frequency—does not fully capture PM's chemical or spatiotemporal complexities. Although a growing number of health studies use modelled exposure estimates, the lack of speciated measurements in some areas hinders the full validation of such methods.

While previous health studies differentiated source-specific events via $PM_{2.5}$ concentration changes (e.g., Table S6), here, chemical composition measurements allowed us to exclusively target wildfire organic aerosols and evaluate source-based health effects. This can be further

enabled by long-term, continuous, and accurate monitoring of the speciated $PM_{2.5}$ measured here (e.g., ASCENT network) in major populated areas to enable future epidemiological studies across different populations and health outcomes. The ensuing scientific evidence on which sources and chemical/physical particle characteristics (e.g., age, oxidation) are most harmful could aid effective decision-making to protect public health, especially as $PM_{2.5}$ reductions have largely stagnated at levels with continued health risks (Hass-Mitchell et al., 2024; Weichenthal et al., 2022). In addition to real-time PM speciation like that leveraged here, characteristics such as potential oxidative stress are not routinely measured in large-scale regulatory networks, further demonstrating the need for additional monitoring and subsequent health analysis.

Additional pressing health-focused research needs include the effects of different fire types (e.g., fuel type, combustion conditions), downwind plume transformations (e.g., oxidation conditions, formation of secondary organic aerosols), key hazardous gas-phase co-pollutants (e.g., formaldehyde; Fig. S9), the impacts of multiple stressors (i.e., repeated exposure to wildfire smoke over multiple events), and different lag times (e.g., same day, weeks or months later).

In all, these observations in summer 2023 clearly established a prominent role for wildfire smoke transport to NYC and other cities largely insulated from wildfire's air quality impacts, with increases in exposure to be expected well beyond the populous Eastern U.S. Therefore, effectively achieving co-benefits for air, climate, and health during ever-expanding wildfire seasons that threaten to setback urban air quality necessitates holistic science and policies to capture the complex multipollutant emissions from wildfires. This includes its relative contributions to air pollution in the context of other sources, oxidative transformations in chemical composition, and multidisciplinary understanding of how these multifaceted pollutant mixtures, including aged aerosols, impact human health over the coming decades.

Methods

Study period selection

The May 15 to June 13, 2023 study period included the major Quebec wildfire smoke transport episode (i.e., June 6-9), as well as several other smoke transport events spanning Western to Eastern Canada. Yet, equally important, this study period allowed us to focus on smoke-related contributions to less- and more-oxidized organic aerosol components prior to the onset of hotter summertime temperatures with more secondary organic aerosol contributions from other temperature-dependent sources and processes, as shown in prior work at the site (Hass-Mitchell et al., 2024). By using this study period, we were able to better isolate the contributions of oxidized transported smoke to the generic oxidized organic aerosol factors across the 5 different smoke events with reduced temperature-related influences compared to during the summer.

Instrumentation, measurement, and field site details

The ASCENT site is located at Queens College (40.74°N, 73.82°W, 16.2-16.6 m above sea level), in one of the New York State Department of Environmental Conservation (NYS DEC) air quality monitoring stations. It is situated on a college campus that is located near an interstate highway and surrounded by a mix of residential and commercial neighborhoods. ASCENT is a new, long-term, advanced aerosol measurement network in the U.S. for advancing knowledge on the impacts

of aerosols on air quality, climate, human health, visibility, and ecosystems (https://ascent.research.gatech.edu/).

The Aerodyne Time-of-Flight Aerosol Chemical Speciation Monitor (ACSM) equipped with a standard vaporizer $PM_{2.5}$ aerodynamic lens was deployed to measure the mass concentration and chemical composition of organic, nitrate, ammonium, sulfate, and chloride aerosol components (Fröhlich et al., 2013; Ng et al., 2011b). The time resolution was set to 10 min per data point, switching between ambient and the filter sampling every 20 sec. Data was processed and analyzed with Tofware v3.3.0, operated in IgorPro 9.0.2.4 (Wavemetrics). The ionization efficiency (IE) for nitrate and relative ionization efficiency (RIE) for sulfate and ammonium were determined by atomizing ammonium nitrate and ammonium sulfate solutions into the ACSM.

The Magee Scientific AE33 aethalometer was used to measure black carbon (BC) and brown carbon (BrC) concentrations. Optical absorption at wavelengths of 370, 470, 520, 590, 660, 880 and 950 nm were measured at the time resolution of 1 min. Absorption at 880 nm was used to determine the BC mass concentrations, assuming a mass absorption cross-section coefficient of 7.77 m^2 g^{-1}. BrC mass concentrations were estimated by subtracting BC from the total absorption at 370 nm and a mass absorption cross-section coefficient of 18.47 m^2 g^{-1} is applied for the conversion. The Sailbri Cooper Xact 625i Ambient Continuous Multi-metal Monitor was used to measure trace metal concentrations at 1-hour resolution. 24 elements (Si, S, Cl, K, Ca, Ti, V, Cr, Mn, Fe, Co, Ni, Cu, Zn, As, Se, Cd, Sn, Sb, Ba, Pt, Hg, Pb, Bi) were measured via X-ray fluorescence (EDXRF) analysis. Scanning Mobility Particle Sizer (SMPS) was used to monitor size-dependent particle number and volume concentrations. The SMPS consists of an Electrostatic Classifier (EC, TSI 3082) and a water-based Condensation Particle Counter (WCPC, TSI 3789).

The ACSM and SMPS shared an inlet and the AE33 and Xact each had dedicated inlets (5.2-5.6 m above ground). ACSM, SMPS, and AE33 were outfitted with $PM_{2.5}$ cyclones (3 and 5 lpm, respectively) and 1/2" OD stainless steel inlets with Nafion dryers to dry the particles (RH<35%). The Xact was equipped with a $PM_{2.5}$ cyclone (16.7 lpm) and 1.25" ID aluminum inlet, followed by a heater to dry particles before the instrument.

In addition to ASCENT instrumentation, a range of criteria pollutants were measured at the Queens College monitoring station. Ozone was measured via Teledyne API T400 ozone analyzer. Nitrogen oxides were measured using total nitrogen oxides (i.e., NO_y) with an inlet mounted catalyst (Thermo Scientific Model 42i-Y NO_y Analyzer) and NO_x (i.e., NO + NO_2) (Thermo Scientific Model 42i-TL TRACE Level NO_x Analyzer). SO_2 was measured via a Thermo Fisher analyzer (TEI 43i - TLE). Carbon monoxide (CO) was measured via a Thermo Fisher analyzer (TEI 48i - TLE). Formaldehyde was unavailable at the Queens College but was measured at the NYS DEC Bronx site via a Picarro G2307 Gas Concentration Analyzer. NYS Mesonet provided meteorological data collected via a Lufft V200A sonic anemometer (Brotzge et al., 2020).

Identification of wildfire-influenced events and background periods

Locations of active fires were identified using the Fire Detection and Characterization (FDC) product from NOAA's Geostationary Operational Environmental Satellite (GOES) system. This system provides 10 min observations over the entire western hemisphere, with an automated active

fire product (at 2 km nominal spatial resolution) built primarily from mid-wave infrared and long-wave infrared data.

Smoke maps were retrieved from the NOAA/NESDIS Satellite Analysis Branch's Hazard Mapping System (HMS), where analysts use GOES true-color imagery available during the sunlit period of orbit to outline smoke polygons. The system assigns qualitative labels of *light*, *medium*, and *heavy* based on the apparent opacity of smoke in the satellite images.

144-hr long backward air-mass trajectories were calculated using the HYSPLIT model at a starting height of 500 m above sea level (Stein et al., 2015). Trajectories were calculated at 1 hr intervals between May 10, 2023 to June 16, 2023 using meteorological data from the GDAS (Global Data Assimilation System) archive, which has global, 3-hr, 1° latitude/longitude meteorological data at 23 pressure surfaces between 1000 hPa and 20 hPa.

For the purposes of enhancement calculations, two distinct background periods were chosen when there were no evident wildfire influences in the speciated PM data or from Hybrid Single Particle Lagrangian Integrated Trajectory (HYSPLIT) backward trajectories and smoke maps (Fig. S10). Still, the backward trajectories cover a broad regional background with similar back trajectories to several of the other smoke events, include similar local urban influences, and were not affected by rain events.

Estimation of wildfire smoke plume transport times

In addition to backward trajectory analysis, we performed forward trajectory analysis using GDAS meteorological data with the HYSPLIT model to estimate the distribution of transport times of the 5 major wildfire smoke transport events (Fig. S2). 144-hr long forward trajectories were initialized from GOES fire detection points at three different heights (500, 1500, and 2500 m) to account for the effect of variabilities in burning conditions and meteorology on plume injection heights (Val Martin et al., 2010), following the methodology from Brey et al. (2018) For each wildfire smoke transport event window, points detected between 144 hr before the start of the event to the end of the event with fire radiative power (FRP) ≥ 250 were selected to construct a list of starting points. Trajectories were initiated at multiple start times to include forward trajectories over the day as burning conditions shift and to account for the influence of sunlight on fire detection. The start time of each trajectory was set to the nearest hour of fire detection time as well as every hour within ±12 hr of the fire detection time (i.e. 25 starting times per fire detection). Duplicate (latitude, longitude, start time) points were then removed from this expanded list of starting points before computing forward trajectories.

Due to the physical, computational, and measurement limitations of the HYSPLIT model, the error in trajectory point location can range from 15% to 30% of the trajectory travel distance (Draxler and Rolph, 2007). To account for this error and retrieve the atmospheric age distribution of transported smoke reaching the measurement site, we included the transport time of trajectory points that distanced within 500 km from the site during the wildfire event window. This approach allowed us to capture both "fresh" and aged smoke reaching the site during each event window. The filtering and plotting of trajectory points was performed using the 'simple features' R package (Pebesma and Bivand, 2023).

Identification of dust and non-dust potassium

While potassium is one of the most abundant metals in biomass burning emissions (e.g., 2-5% by particle mass) (Reid et al., 2005) and thus has been previously used as a tracer of wildfire events, (Andreae, 1983; Li et al., 2003; Sullivan et al., 2008; Pachon et al., 2013) it can also originate from mineral dust or coal combustion (if used in the study region). (Finkelman, 1999; Chow et al., 2003; Thorpe and Harrison, 2008) To apportion potassium from biomass burning, we performed linear regressions on potassium with other trace metals during background periods to estimate mineral dust potassium and subtract it. Five metals (Ca, Fe, Ti, Cu, Ba), which were confirmed to have weak correlations with potassium during the extreme smoke event (June 6-9 Quebec wildfire smoke episode) (Fig. S11), were investigated as possible candidates for resolving mineral dust potassium. The ratios of these metals to potassium have also been utilized to identify different sources of mineral dust elsewhere (Liu et al., 2022; Apeagyei et al., 2011; Yu et al., 2018; Pachon et al., 2013).

For all points measured during the background period, linear regression analysis was performed on potassium against each of the five selected metals to obtain unique site-specific prediction equations for the concentration of potassium from mineral dust (Fig. S12). Mean values of predictor metal species during each event were then used to estimate the corresponding mean amount of mineral dust potassium. The results of this approach in Fig. S13 show that when using the different predictor metals, the predicted concentration of mineral dust potassium remains similar across both the wildfire smoke events as well as the average potassium concentration measured during the background events. Contributions from coal combustion in our study region are expected to be minimal as U.S. coal combustion has undergone steep declines since 2008, and furthermore particle lead concentrations, which can be a coal combustion tracer (Yu et al., 2018), was only detected in 5.1% of hourly data points during the study period (MDL: 0.22 ng m^{-3}).

We note that trace metal species utilized for the background mineral dust estimation can be affected by other factors: resuspension of trace metals in soil by wildfires (Isley and Taylor, 2020), local activities, and other emission sources. Thus, the proper identification of background periods using meteorology and gas-phase/aerosol measurements alongside a comprehensive understanding regarding sources of metal emissions upwind of the measurement site is imperative for applying this approach.

Source apportionment of organic aerosols via positive matrix factorization

Positive matrix factorization (PMF) analysis was performed on the organic aerosol spectral matrix (*m/z* 12-100) obtained from the ACSM, using the PMF Evaluation Toolkit (PET v.3.08) to determine the source contributions of organic aerosol source types. PMF solves bilinear unmixing problems via a least-squares approach, which is based on a receptor-only multivariate factor analytic model. PMF deconvolves the organic aerosol data matrix as a linear combination of multiple factors with constant mass spectra while varying concentrations. PMF solutions are examined following the procedures in Zhang et al. (2011) The optimal solution was determined after examining the residuals of PMF fits, diurnal trends of each factor, known-tracer ion signatures of factor mass spectra, and correlations with external tracers. The rotational ambiguity of PMF solutions was examined by changing FPEAK. An FPEAK value of -0.2 was chosen based on the tracer ion signatures and correlation with external tracers. This solution resolved an aged

biomass burning organic aerosol (BBOA) factor that significantly contributed to organic aerosols from June 10 to 13, when the aged Quebec wildfire plume arrived after being transported over the Atlantic Ocean (Fig. S2). Using this solution, the aged BBOA factor included biomass burning tracer ions (*m/z* 60, 73) but with a greater extent of aging (e.g., higher f_{44} and OSc) than the fresh biomass burning factor (BBOA). Additionally, the FPEAK = -0.2 solution better resolved HOA and COA factors with improved separation from the other factors, and a more typical COA and HOA temporal variation (e.g., diurnal patterns) and mass spectra for COA (i.e., f_{55}/f_{57}). Key diagnostic plots were shown in Fig. S14.

We resolved six factors from the organic aerosols: more-oxidized oxygenated organic aerosols (MO-OOA), less-oxidized OOA (LO-OOA), BBOA, aged-BBOA (aBBOA), hydrocarbon-like organic aerosols (HOA), and cooking organic aerosols (COA) (Fig. S5). MO-OOA and LO-OOA were relatively more oxidized compared to the other factors and were differentiated by relative fractions of *m/z* 43 and 44 (Ng et al., 2011a). BBOA and aBBOA have enhanced signals at *m/z* 60 and 73. HOA includes a morning commute maxima and enhanced signals at *m/z* 55 and 57. COA is determined by prominent signals at *m/z* 41 and 55 with a higher f_{55}-to-f_{57} ratio than that of HOA with elevated concentration at around lunch and dinner times. Other than BBOA and aBBOA, the types of organic aerosol factors apportioned in this study are consistent with a previous study performed at the same location during the previous summer (without major wildfire activity) (Hass-Mitchell et al., 2024).

Monte Carlo estimates of potential oxidative stress enhancements

Potential oxidative stress enhancements for each of the five major wildfire smoke transport events were estimated via a Monte Carlo analysis (N=1×10^6) with input values adopted from multiple prior studies that utilized assay-based observations of oxidative stress associated with PMF-derived source factors and/or degree of oxidation. Relative enhancements (%) for each event were determined by estimating the potential oxidative stress resulting from $PM_{2.5}$ during each smoke episode (Eqn. 1) in comparison to that estimated during the average of the two background periods (Eqn. 2). We adopted a series of coefficients ($\alpha_{i,k}$) based on the findings of six different studies in the literature that attributed observed oxidative stress across organic aerosol source types or based on degree of oxidation (Table S7) (Liu et al., 2023; Daellenbach et al., 2020; Zhou et al., 2019; Tuet et al., 2017; Yu et al., 2022; Verma et al., 2015), and we employed them in the following equations.

$$Potential\ Oxidative\ Stress_{x,i} = \sum_k (\alpha_{i,k} * gnoise(0.2) * S_k) \qquad \text{(Equation 1)}$$

$$\Delta Potential\ Oxidative\ Stress = \frac{POS_{Smoke\ Episode\ \#} - POS_{Background}}{POS_{Background}} \qquad \text{(Equation 2)}$$

Where Eqn. 1 sums the potential oxidative stress resulting from each smoke episode-averaged PMF factor (S_k) for each factor type k (e.g., MO-OOA), and i represents the randomly chosen (i.e., L'Ecuyer with added Bayes-Durham shuffle in IgorPro) literature scenario from Table S7, which contains the weighting coefficients for each PMF factor ($\alpha_{i,k}$) based on scenarios from each of the applicable studies. In each iteration of the Monte Carlo analysis, the potential oxidative stress for each PMF factor was estimated by multiplying the oxidative stress coefficients of each organic aerosol factor ($\alpha_{i,k}$) with uncertainty fitting ±20% Gaussian-distributed noise (*gnoise*(0.2)), which was multiplied by the episode-averaged organic aerosol contribution for each source factor

obtained via PMF analysis (S_k) (Table S3). Then, these values are summed (Eqn. 1) for both the smoke event and the background period and the relative difference was determined via Eqn. 2. Other uncertainty ranges spanning from ±10% to ±50% were tested and are shown in Fig. S8.

This analysis was designed to be as inclusive of prior work and as possible, noting that prior studies on PM toxicity of organic aerosol source types/factors use different oxidative stress estimation methods and contain a varying mix of source factors. For example, the adopted literature coefficients from the literature used two different methods to measure the indicators of oxidative stress from PM exposure: acellular and cellular assays. Acellular (chemical-based) assays were used to measure oxidative potential (via dithiothreitol, ascorbic acid, and dichlorofluorescin assays) (Daellenbach et al., 2020; Yu et al., 2022; Verma et al., 2015) or intracellular/particle-bound reactive oxygen species (via dichlorofluorescin assay) (Zhou et al., 2019). Meanwhile, cellular assays were used to measure both chemically and biologically generated reactive oxygen species (via alveolar macrophage assay) (Tuet et al., 2017; Liu et al., 2023). Furthermore, in prior work using ambient data (Daellenbach et al., 2020; Liu et al., 2023; Yu et al., 2022; Zhou et al., 2019; Verma et al., 2015), multiple linear regression models were used (in those studies) to quantify associations (i.e., α) between observed oxidative stress and PM composition (e.g., PMF source factors derived from AMS data). Whereas, Tuet et al. (2017) examined oxidative stress as a function of degree of oxidation. They are all used here in Table S7 to provide the $\alpha_{i,k}$ coefficients, which are normalized to avoid bias when cross-comparing across studies (i.e., secondary approach below). While the specific assays and methods vary across these studies, the units of $\alpha_{i,k}$ represent quantity of oxidative stress per μg m^{-3} of a given PMF source factor (S_k).

A Monte Carlo approach is specifically employed here given the uncertainties associated with estimating the potential oxidative stress from each of the smoke episodes based on the available studies. It is focused on the oxidative stress associated with the organic aerosols and does not include coincident enhancements of redox-active metals (i.e., Mn, Fe, Cu) (Table S4), which would likely increase estimates of the generation or reactive oxygen species (Liu et al., 2023; Lakey et al., 2016). Given the varying methods employed across the applicable prior work, the results of Monte Carlo analysis are presented as the percentage (%) enhancements and not as absolute enhancements. In a sensitivity analysis, we tested two different approaches for choosing potential oxidative stress coefficients across the studies. In the first and main approach (Fig. 3), the potential oxidative stress calculated in Eqn. 1 for background and wildfire periods were determined using the same scenario i in each Monte Carlo iteration. In the secondary approach, the potential oxidative stress for background and wildfire periods used randomly varying scenarios i in each Monte Carlo iteration. This second approach yielded consistent results with similar median values across the varying uncertainty cases (Fig. S8), and an expectedly broader spread in results given the study-to-study variations in methods, assays, and study designs.

In all, the Monte Carlo analysis captures the enhancements in oxidative stress across the five wildfire events by mapping the cellular or acellular results from prior work to the observed source factors in this study. We acknowledge the prior studies have $PM_{2.5}$ compositional differences relative to this work as most of the studies were not predominantly focused on oxidized biomass burning related organic aerosols and all were at different locations. Yet, our findings highlight the key role that oxidation plays in enhancing oxidative stress (consistent with Tuet et al. (2017) and Liu et al. (2023)) and emphasizes the uncertainty and important future reach priorities around the relative impacts of fresh vs. highly-aged biomass burning organic aerosols.

Epidemiological Analysis

We evaluated the risks associated with the wildfire events over the course of the study period via investigating changes in the number of daily emergency department (ED) visits of asthma in NYC against the chemically-resolved PM data and source apportionment results. Temporal variations in biomass burning organic aerosols, the sum of smoke-related organic aerosol contributions (BBOA + aBBOA + LO-OOA + MO-OOA), and potassium were assessed as the exposures. The outcome variable was the daily asthma ED visits in NYC obtained from the EpiQuery – Syndromic Surveillance data, which provided data reported by 53 emergency departments in NYC to the New York Health Department (New York City Department of Health and Mental Hygiene. Epiquery - [Syndromic Surveillance Data 2023]. [Accessed on September 26, 2023). For each day, this surveillance provided nearly real-time data on the daily number of ED visits for target acute diseases until 2 prior days. The number of daily ED visits for asthma-related symptom (asthma, wheezing, complaint in airway, or chronic obstructive pulmonary disorder) from May 15 to June 13, 2023 was classified into six age groups: all ages, 0–4 years, 5–7 years, 0–17 years, 18–64 years, and ≥65 years. We applied a time-dependent model based on a generalized additive model as follows (Zeger et al., 2006; Bhaskaran et al., 2013):

$$ln[E(Y_t)] = \beta_0 + \beta_1 P_t + \beta_2 DOW_t + \beta_3 FED_t + s(Time_t, 4) \quad \text{(Equation 3)}$$

Where $ln[E(Y_t)]$ is the expected number of age-specific asthma ED visits on day t, β_0 is the model intercept, and P_t is concentration of the input parameter (i.e., separate models for K, BBOA only, and BBOA + aBBOA + LO-OOA + MO-OOA) on day t. The models considered potential confounding effects from temporal trends ($Time_t$), day of the week (DOW_t), and federal holidays (Fed_t). A natural spline function with 4 degrees of freedom (df) was applied for the temporal trend. The risk estimation was represented as the estimated percent change of daily number of ED visits for an interquartile range (IQR) increase in concentration of exposure (i.e., [exp(IQR*β1)-1]*100). The models were also separately applied for each age group.

References

Abatzoglou, J. T. and Williams, A. P.: Impact of anthropogenic climate change on wildfire across western US forests, Proceedings of the National Academy of Sciences, 113, 11770-11775, 10.1073/pnas.1607171113, 2016.

Andreae, M. O.: Soot Carbon and Excess Fine Potassium: Long-Range Transport of Combustion-Derived Aerosols, Science, 220, 1148-1151, 10.1126/science.220.4602.1148, 1983.

Apeagyei, E., Bank, M. S., and Spengler, J. D.: Distribution of heavy metals in road dust along an urban-rural gradient in Massachusetts, Atmospheric Environment, 45, 2310-2323, 10.1016/j.atmosenv.2010.11.015, 2011.

Bhaskaran, K., Gasparrini, A., Hajat, S., Smeeth, L., and Armstrong, B.: Time series regression studies in environmental epidemiology, International Journal of Epidemiology, 42, 1187-1195, 10.1093/ije/dyt092, 2013.

Bourgeois, I., Peischl, J., Neuman, J. A., Brown, S. S., Thompson, C. R., Aikin, K. C., Allen, H. M., Angot, H., Apel, E. C., Baublitz, C. B., Brewer, J. F., Campuzano-Jost, P., Commane, R., Crounse, J. D., Daube, B. C., DiGangi, J. P., Diskin, G. S., Emmons, L. K., Fiore, A. M., Gkatzelis, G. I., Hills, A., Hornbrook, R. S., Huey, L. G., Jimenez, J. L.,

Kim, M., Lacey, F., McKain, K., Murray, L. T., Nault, B. A., Parrish, D. D., Ray, E., Sweeney, C., Tanner, D., Wofsy, S. C., and Ryerson, T. B.: Large contribution of biomass burning emissions to ozone throughout the global remote troposphere, Proceedings of the National Academy of Sciences, 118, e2109628118, 10.1073/pnas.2109628118, 2021.

Brey, S. J., Ruminski, M., Atwood, S. A., and Fischer, E. V.: Connecting smoke plumes to sources using Hazard Mapping System (HMS) smoke and fire location data over North America, Atmos. Chem. Phys., 18, 1745-1761, 10.5194/acp-18-1745-2018, 2018.

Brotzge, J. A., Wang, J., Thorncroft, C. D., Joseph, E., Bain, N., Bassill, N., Farruggio, N., Freedman, J. M., Hemker, K., Johnston, D., Kane, E., McKim, S., Miller, S. D., Minder, J. R., Naple, P., Perez, S., Schwab, J. J., Schwab, M. J., and Sicker, J.: A Technical Overview of the New York State Mesonet Standard Network, Journal of Atmospheric and Oceanic Technology, 37, 1827-1845, https://doi.org/10.1175/JTECH-D-19-0220.1, 2020.

Burke, M., Childs, M. L., de la Cuesta, B., Qiu, M., Li, J., Gould, C. F., Heft-Neal, S., and Wara, M.: The contribution of wildfire to PM2.5 trends in the USA, Nature, 622, 761-766, 10.1038/s41586-023-06522-6, 2023.

Chen, K., Ma, Y., Bell, M. L., and Yang, W.: Canadian Wildfire Smoke and Asthma Syndrome Emergency Department Visits in New York City, JAMA, 330, 1385-1387, 10.1001/jama.2023.18768, 2023.

Chow, J. C., Watson, J. G., Ashbaugh, L. L., and Magliano, K. L.: Similarities and differences in PM10 chemical source profiles for geological dust from the San Joaquin Valley, California, Atmospheric Environment, 37, 1317-1340, https://doi.org/10.1016/S1352-2310(02)01021-X, 2003.

Coggon, M. M., Lim, C. Y., Koss, A. R., Sekimoto, K., Yuan, B., Gilman, J. B., Hagan, D. H., Selimovic, V., Zarzana, K. J., Brown, S. S., Roberts, J. M., Müller, M., Yokelson, R., Wisthaler, A., Krechmer, J. E., Jimenez, J. L., Cappa, C., Kroll, J. H., de Gouw, J., and Warneke, C.: OH chemistry of non-methane organic gases (NMOGs) emitted from laboratory and ambient biomass burning smoke: evaluating the influence of furans and oxygenated aromatics on ozone and secondary NMOG formation, Atmos. Chem. Phys., 19, 14875-14899, 10.5194/acp-19-14875-2019, 2019.

Cubison, M. J., Ortega, A. M., Hayes, P. L., Farmer, D. K., Day, D., Lechner, M. J., Brune, W. H., Apel, E., Diskin, G. S., Fisher, J. A., Fuelberg, H. E., Hecobian, A., Knapp, D. J., Mikoviny, T., Riemer, D., Sachse, G. W., Sessions, W., Weber, R. J., Weinheimer, A. J., Wisthaler, A., and Jimenez, J. L.: Effects of aging on organic aerosol from open biomass burning smoke in aircraft and laboratory studies, Atmos. Chem. Phys., 11, 12049-12064, 10.5194/acp-11-12049-2011, 2011.

Daellenbach, K. R., Uzu, G., Jiang, J., Cassagnes, L.-E., Leni, Z., Vlachou, A., Stefenelli, G., Canonaco, F., Weber, S., Segers, A., Kuenen, J. J. P., Schaap, M., Favez, O., Albinet, A., Aksoyoglu, S., Dommen, J., Baltensperger, U., Geiser, M., El Haddad, I., Jaffrezo, J.-L., and Prévôt, A. S. H.: Sources of particulate-matter air pollution and its oxidative potential in Europe, Nature, 587, 414-419, 10.1038/s41586-020-2902-8, 2020.

Draxler, R. R. and Rolph, G. D.: HYSPLIT-WEB Short Course, 2007.

Finkelman, R. B.: Trace elements in coal, Biological Trace Element Research, 67, 197-204, 10.1007/BF02784420, 1999.

Fröhlich, R., Cubison, M. J., Slowik, J. G., Bukowiecki, N., Prévôt, A. S. H., Baltensperger, U., Schneider, J., Kimmel, J. R., Gonin, M., Rohner, U., Worsnop, D. R., and Jayne, J. T.: The ToF-ACSM: a portable aerosol chemical speciation monitor with TOFMS detection, Atmos. Meas. Tech., 6, 3225-3241, 10.5194/amt-6-3225-2013, 2013.

Hass-Mitchell, T., Joo, T., Rogers, M., Nault, B. A., Soong, C., Tran, M., Seo, M., Machesky, J. E., Canagaratna, M., Roscioli, J., Claflin, M. S., Lerner, B. M., Blomdahl, D. C., Misztal, P. K., Ng, N. L., Dillner, A. M., Bahreini, R., Russell, A., Krechmer, J. E., Lambe, A., and Gentner, D. R.: Increasing Contributions of Temperature-Dependent Oxygenated Organic Aerosol to Summertime Particulate Matter in New York City, ACS ES&T Air, 1, 113-128, 10.1021/acsestair.3c00037, 2024.

Hatch, L. E., Luo, W., Pankow, J. F., Yokelson, R. J., Stockwell, C. E., and Barsanti, K. C.: Identification and quantification of gaseous organic compounds emitted from biomass burning using two-dimensional gas chromatography–time-of-flight mass spectrometry, Atmos. Chem. Phys., 15, 1865-1899, 10.5194/acp-15-1865-2015, 2015.

Hayden, K. L., Li, S. M., Liggio, J., Wheeler, M. J., Wentzell, J. J. B., Leithead, A., Brickell, P., Mittermeier, R. L., Oldham, Z., Mihele, C. M., Staebler, R. M., Moussa, S. G., Darlington, A., Wolde, M., Thompson, D., Chen, J., Griffin, D., Eckert, E., Ditto, J. C., He, M., and Gentner, D. R.: Reconciling the total carbon budget for boreal forest wildfire emissions using airborne observations, Atmos. Chem. Phys., 22, 12493-12523, 10.5194/acp-22-12493-2022, 2022.

Hecobian, A., Liu, Z., Hennigan, C. J., Huey, L. G., Jimenez, J. L., Cubison, M. J., Vay, S., Diskin, G. S., Sachse, G. W., Wisthaler, A., Mikoviny, T., Weinheimer, A. J., Liao, J., Knapp, D. J., Wennberg, P. O., Kürten, A., Crounse, J. D., Clair, J. S., Wang, Y., and Weber, R. J.: Comparison of chemical characteristics of 495 biomass burning plumes intercepted by the NASA DC-8 aircraft during the ARCTAS/CARB-2008 field campaign, Atmos. Chem. Phys., 11, 13325-13337, 10.5194/acp-11-13325-2011, 2011.

Hems, R. F., Schnitzler, E. G., Liu-Kang, C., Cappa, C. D., and Abbatt, J. P. D.: Aging of Atmospheric Brown Carbon Aerosol, ACS Earth and Space Chemistry, 5, 722-748, 10.1021/acsearthspacechem.0c00346, 2021.

Hinds, W. C.: Aerosol technology: properties, behavior, and measurement of airborne particles, John Wiley & Sons1999.

Hodshire, A. L., Bian, Q., Ramnarine, E., Lonsdale, C. R., Alvarado, M. J., Kreidenweis, S. M., Jathar, S. H., and Pierce, J. R.: More Than Emissions and Chemistry: Fire Size, Dilution, and Background Aerosol Also Greatly Influence Near-Field Biomass Burning Aerosol Aging, Journal of Geophysical Research: Atmospheres, 124, 5589-5611, https://doi.org/10.1029/2018JD029674, 2019a.

Hodshire, A. L., Akherati, A., Alvarado, M. J., Brown-Steiner, B., Jathar, S. H., Jimenez, J. L., Kreidenweis, S. M., Lonsdale, C. R., Onasch, T. B., Ortega, A. M., and Pierce, J. R.: Aging Effects on Biomass Burning Aerosol Mass and Composition: A Critical Review of Field and Laboratory Studies, Environmental Science & Technology, 53, 10007-10022, 10.1021/acs.est.9b02588, 2019b.

Isley, C. F. and Taylor, M. P.: Atmospheric remobilization of natural and anthropogenic contaminants during wildfires, Environ Pollut, 267, 115400, 10.1016/j.envpol.2020.115400, 2020.

Jen, C. N., Hatch, L. E., Selimovic, V., Yokelson, R. J., Weber, R., Fernandez, A. E., Kreisberg, N. M., Barsanti, K. C., and Goldstein, A. H.: Speciated and total emission factors of

particulate organics from burning western US wildland fuels and their dependence on combustion efficiency, Atmos. Chem. Phys., 19, 1013-1026, 10.5194/acp-19-1013-2019, 2019.

Jimenez, J. L., Canagaratna, M. R., Donahue, N. M., Prevot, A. S. H., Zhang, Q., Kroll, J. H., DeCarlo, P. F., Allan, J. D., Coe, H., Ng, N. L., Aiken, A. C., Docherty, K. S., Ulbrich, I. M., Grieshop, A. P., Robinson, A. L., Duplissy, J., Smith, J. D., Wilson, K. R., Lanz, V. A., Hueglin, C., Sun, Y. L., Tian, J., Laaksonen, A., Raatikainen, T., Rautiainen, J., Vaattovaara, P., Ehn, M., Kulmala, M., Tomlinson, J. M., Collins, D. R., Cubison, M. J., Dunlea, J., Huffman, J. A., Onasch, T. B., Alfarra, M. R., Williams, P. I., Bower, K., Kondo, Y., Schneider, J., Drewnick, F., Borrmann, S., Weimer, S., Demerjian, K., Salcedo, D., Cottrell, L., Griffin, R., Takami, A., Miyoshi, T., Hatakeyama, S., Shimono, A., Sun, J. Y., Zhang, Y. M., Dzepina, K., Kimmel, J. R., Sueper, D., Jayne, J. T., Herndon, S. C., Trimborn, A. M., Williams, L. R., Wood, E. C., Middlebrook, A. M., Kolb, C. E., Baltensperger, U., and Worsnop, D. R.: Evolution of Organic Aerosols in the Atmosphere, Science, 326, 1525-1529, 10.1126/science.1180353, 2009.

Jolleys, M. D., Coe, H., McFiggans, G., Capes, G., Allan, J. D., Crosier, J., Williams, P. I., Allen, G., Bower, K. N., Jimenez, J. L., Russell, L. M., Grutter, M., and Baumgardner, D.: Characterizing the Aging of Biomass Burning Organic Aerosol by Use of Mixing Ratios: A Meta-analysis of Four Regions, Environmental Science & Technology, 46, 13093-13102, 10.1021/es302386v, 2012.

Joo, T., Rivera-Rios, J. C., Takeuchi, M., Alvarado, M. J., and Ng, N. L.: Secondary Organic Aerosol Formation from Reaction of 3-Methylfuran with Nitrate Radicals, ACS Earth and Space Chemistry, 3, 922-934, 10.1021/acsearthspacechem.9b00068, 2019.

Joo, T., Machesky, J. E., Zeng, L., Hass-Mitchell, T., Weber, R. J., Gentner, D. R., and Ng, N. L.: Secondary Brown Carbon Formation From Photooxidation of Furans From Biomass Burning, Geophysical Research Letters, 51, e2023GL104900, https://doi.org/10.1029/2023GL104900, 2024.

Joo, T., Chen, Y., Xu, W., Croteau, P., Canagaratna, M. R., Gao, D., Guo, H., Saavedra, G., Kim, S. S., Sun, Y., Weber, R., Jayne, J., and Ng, N. L.: Evaluation of a New Aerosol Chemical Speciation Monitor (ACSM) System at an Urban Site in Atlanta, GA: The Use of Capture Vaporizer and PM2.5 Inlet, ACS Earth and Space Chemistry, 5, 2565-2576, 10.1021/acsearthspacechem.1c00173, 2021.

Koss, A. R., Sekimoto, K., Gilman, J. B., Selimovic, V., Coggon, M. M., Zarzana, K. J., Yuan, B., Lerner, B. M., Brown, S. S., Jimenez, J. L., Krechmer, J., Roberts, J. M., Warneke, C., Yokelson, R. J., and de Gouw, J.: Non-methane organic gas emissions from biomass burning: identification, quantification, and emission factors from PTR-ToF during the FIREX 2016 laboratory experiment, Atmos. Chem. Phys., 18, 3299-3319, 10.5194/acp-18-3299-2018, 2018.

Lakey, P. S. J., Berkemeier, T., Tong, H., Arangio, A. M., Lucas, K., Pöschl, U., and Shiraiwa, M.: Chemical exposure-response relationship between air pollutants and reactive oxygen species in the human respiratory tract, Scientific Reports, 6, 32916, 10.1038/srep32916, 2016.

Li, J., Pósfai, M., Hobbs, P. V., and Buseck, P. R.: Individual aerosol particles from biomass burning in southern Africa: 2, Compositions and aging of inorganic particles, Journal of Geophysical Research: Atmospheres, 108, https://doi.org/10.1029/2002JD002310, 2003.

Liang, Y., Weber, R. J., Misztal, P. K., Jen, C. N., and Goldstein, A. H.: Aging of Volatile Organic Compounds in October 2017 Northern California Wildfire Plumes, Environmental Science & Technology, 56, 1557-1567, 10.1021/acs.est.1c05684, 2022.

Lim, C. Y., Hagan, D. H., Coggon, M. M., Koss, A. R., Sekimoto, K., de Gouw, J., Warneke, C., Cappa, C. D., and Kroll, J. H.: Secondary organic aerosol formation from the laboratory oxidation of biomass burning emissions, Atmos. Chem. Phys., 19, 12797-12809, 10.5194/acp-19-12797-2019, 2019.

Liu, F., Joo, T., Ditto, J. C., Saavedra, M. G., Takeuchi, M., Boris, A. J., Yang, Y., Weber, R. J., Dillner, A. M., Gentner, D. R., and Ng, N. L.: Oxidized and Unsaturated: Key Organic Aerosol Traits Associated with Cellular Reactive Oxygen Species Production in the Southeastern United States, Environmental Science & Technology, 57, 14150-14161, 10.1021/acs.est.3c03641, 2023.

Liu, X., Turner, J. R., Hand, J. L., Schichtel, B. A., and Martin, R. V.: A Global-Scale Mineral Dust Equation, J Geophys Res Atmos, 127, e2022JD036937, 10.1029/2022JD036937, 2022.

Masselot, P., Sera, F., Schneider, R., Kan, H., Lavigne, É., Stafoggia, M., Tobias, A., Chen, H., Burnett, R. T., Schwartz, J., Zanobetti, A., Bell, M. L., Chen, B.-Y., Guo, Y.-L. L., Ragettli, M. S., Vicedo-Cabrera, A. M., Åström, C., Forsberg, B., Íñiguez, C., Garland, R. M., Scovronick, N., Madureira, J., Nunes, B., De la Cruz Valencia, C., Hurtado Diaz, M., Honda, Y., Hashizume, M., Ng, C. F. C., Samoli, E., Katsouyanni, K., Schneider, A., Breitner, S., Ryti, N. R. I., Jaakkola, J. J. K., Maasikmets, M., Orru, H., Guo, Y., Valdés Ortega, N., Matus Correa, P., Tong, S., and Gasparrini, A.: Differential Mortality Risks Associated With PM2.5 Components: A Multi-Country, Multi-City Study, Epidemiology, 33, 2022.

McArdle, C. E., Dowling, T. C., Carey, K., DeVies, J., Johns, D., Gates, A. L., Stein, Z., Santen, K. L. v., Radhakrishnan, L., Kite-Powell, A., Soetebier, K., Sacks, J. D., Sircar, K., Hartnett, K. P., and Mirabelli, M. C.: Asthma-Associated Emergency Department Visits During the Canadian Wildfire Smoke Episodes — United States, April– August 2023, U.S. Department of Health and Human Services, MMWR and Morbidity and Mortality Weekly Report 926-9352, http://dx.doi.org/10.15585/mmwr.mm7234a5, 2023.

Meek, H. C., Aydin-Ghormoz, H., Bush, K., Muscatiello, N., McArdle, C. E., Weng, C. X., Hoefer, D., Hsu, W.-H., and Rosenberg, E. S.: Notes from the Field: Asthma-Associated Emergency Department Visits During a Wildfire Smoke Event — New York, June 2023, U.S. Department of Health and Human Services, MMWR and Morbidity and Mortality Weekly Report, 933-935, http://dx.doi.org/10.15585/mmwr.mm7234a6, 2023.

Murray, C. J. L. and Aravkin, A. Y. and Zheng, P. and Abbafati, C. and Abbas, K. M. and Abbasi-Kangevari, M. and Abd-Allah, F. and Abdelalim, A. and Abdollahi, M. and Abdollahpour, I. and Abegaz, K. H. and Abolhassani, H. and Aboyans, V. and Abreu, L. G. and Abrigo, M. R. M. and Abualhasan, A. and Abu-Raddad, L. J. and Abushouk, A. I. and Adabi, M. and Adekanmbi, V. and Adeoye, A. M. and Adetokunboh, O. O. and Adham, D. and Advani, S. M. and Agarwal, G. and Aghamir, S. M. K. and Agrawal, A. and Ahmad, T. and Ahmadi, K. and Ahmadi, M. and Ahmadieh, H. and Ahmed, M. B. and Akalu, T. Y. and Akinyemi, R. O. and Akinyemiju, T. and Akombi, B. and Akunna, C. J. and Alahdab, F. and Al-Aly, Z. and Alam, K. and Alam, S. and Alam, T. and Alanezi, F. M. and Alanzi, T. M. and Alemu, B. w. and Alhabib, K. F. and Ali, M. and Ali, S. and Alicandro, G. and Alinia, C. and Alipour, V. and Alizade, H. and Aljunid, S.

M. and Alla, F. and Allebeck, P. and Almasi-Hashiani, A. and Al-Mekhlafi, H. M. and Alonso, J. and Altirkawi, K. A. and Amini-Rarani, M. and Amiri, F. and Amugsi, D. A. and Ancuceanu, R. and Anderlini, D. and Anderson, J. A. and Andrei, C. L. and Andrei, T. and Angus, C. and Anjomshoa, M. and Ansari, F. and Ansari-Moghaddam, A. and Antonazzo, I. C. and Antonio, C. A. T. and Antony, C. M. and Antriyandarti, E. and Anvari, D. and Anwer, R. and Appiah, S. C. Y. and Arabloo, J. and Arab-Zozani, M. and Ariani, F. and Armoon, B. and Ärnlöv, J. and Arzani, A. and Asadi-Aliabadi, M. and Asadi-Pooya, A. A. and Ashbaugh, C. and Assmus, M. and Atafar, Z. and Atnafu, D. D. and Atout, M. M. d. W. and Ausloos, F. and Ausloos, M. and Ayala Quintanilla, B. P. and Ayano, G. and Ayanore, M. A. and Azari, S. and Azarian, G. and Azene, Z. N. and Badawi, A. and Badiye, A. D. and Bahrami, M. A. and Bakhshaei, M. H. and Bakhtiari, A. and Bakkannavar, S. M. and Baldasseroni, A. and Ball, K. and Ballew, S. H. and Balzi, D. and Banach, M. and Banerjee, S. K. and Bante, A. B. and Baraki, A. G. and Barker-Collo, S. L. and Bärnighausen, T. W. and Barrero, L. H. and Barthelemy, C. M. and Barua, L. and Basu, S. and Baune, B. T. and Bayati, M. and Becker, J. S. and Bedi, N. and Beghi, E. and Béjot, Y. and Bell, M. L. and Bennitt, F. B. and Bensenor, I. M. and Berhe, K. and Berman, A. E. and Bhagavathula, A. S. and Bhageerathy, R. and Bhala, N. and Bhandari, D. and Bhattacharyya, K. and Bhutta, Z. A. and Bijani, A. and Bikbov, B. and Bin Sayeed, M. S. and Biondi, A. and Birihane, B. M. and Bisignano, C. and Biswas, R. K. and Bitew, H. and Bohlouli, S. and Bohluli, M. and Boon-Dooley, A. S. and Borges, G. and Borzì, A. M. and Borzouei, S. and Bosetti, C. and Boufous, S. and Braithwaite, D. and Breitborde, N. J. K. and Breitner, S. and Brenner, H. and Briant, P. S. and Briko, A. N. and Briko, N. I. and Britton, G. B. and Bryazka, D. and Bumgarner, B. R. and Burkart, K. and Burnett, R. T. and Burugina Nagaraja, S. and Butt, Z. A. and Caetano dos Santos, F. L. and Cahill, L. E. and Cámera, L. L. A. A. and Campos-Nonato, I. R. and Cárdenas, R. and Carreras, G. and Carrero, J. J. and Carvalho, F. and Castaldelli-Maia, J. M. and Castañeda-Orjuela, C. A. and Castelpietra, G. and Castro, F. and Causey, K. and Cederroth, C. R. and Cercy, K. M. and Cerin, E. and Chandan, J. S. and Chang, K.-L. and Charlson, F. J. and Chattu, V. K. and Chaturvedi, S. and Cherbuin, N. and Chimed-Ochir, O. and Cho, D. Y. and Choi, J.-Y. J. and Christensen, H. and Chu, D.-T. and Chung, M. T. and Chung, S.-C. and Cicuttini, F. M. and Ciobanu, L. G. and Cirillo, M. and Classen, T. K. D. and Cohen, A. J. and Compton, K. and Cooper, O. R. and Costa, V. M. and Cousin, E. and Cowden, R. G. and Cross, D. H. and Cruz, J. A. and Dahlawi, S. M. A. and Damasceno, A. A. M. and Damiani, G. and Dandona, L. and Dandona, R. and Dangel, W. J. and Danielsson, A.-K. and Dargan, P. I. and Darwesh, A. M. and Daryani, A. and Das, J. K. and Das Gupta, R. and das Neves, J. and Dávila-Cervantes, C. A. and Davitoiu, D. V. and De Leo, D. and Degenhardt, L. and DeLang, M. and Dellavalle, R. P. and Demeke, F. M. and Demoz, G. T. and Demsie, D. G. and Denova-Gutiérrez, E. and Dervenis, N. and Dhungana, G. P. and Dianatinasab, M. and Dias da Silva, D. and Diaz, D. and Dibaji Forooshani, Z. S. and Djalalinia, S. and Do, H. T. and Dokova, K. and Dorostkar, F. and Doshmangir, L. and Driscoll, T. R. and Duncan, B. B. and Duraes, A. R. and Eagan, A. W. and Edvardsson, D. and El Nahas, N. and El Sayed, I. and El Tantawi, M. and Elbarazi, I. and Elgendy, I. Y. and El-Jaafary, S. I. and Elyazar, I. R. F. and Emmons-Bell, S. and Erskine, H. E. and Eskandarieh, S. and Esmaeilnejad, S. and Esteghamati, A. and Estep, K. and Etemadi, A. and Etisso, A. E. and Fanzo, J. and Farahmand, M. and Fareed, M. and Faridnia, R. and Farioli, A. and

Faro, A. and Faruque, M. and Farzadfar, F. and Fattahi, N. and Fazlzadeh, M. and Feigin, V. L. and Feldman, R. and Fereshtehnejad, S.-M. and Fernandes, E. and Ferrara, G. and Ferrari, A. J. and Ferreira, M. L. and Filip, I. and Fischer, F. and Fisher, J. L. and Flor, L. S. and Foigt, N. A. and Folayan, M. O. and Fomenkov, A. A. and Force, L. M. and Foroutan, M. and Franklin, R. C. and Freitas, M. and Fu, W. and Fukumoto, T. and Furtado, J. M. and Gad, M. M. and Gakidou, E. and Gallus, S. and Garcia-Basteiro, A. L. and Gardner, W. M. and Geberemariyam, B. S. and Gebreslassie, A. A. A. A. and Geremew, A. and Gershberg Hayoon, A. and Gething, P. W. and Ghadimi, M. and Ghadiri, K. and Ghaffarifar, F. and Ghafourifard, M. and Ghamari, F. and Ghashghaee, A. and Ghiasvand, H. and Ghith, N. and Gholamian, A. and Ghosh, R. and Gill, P. S. and Ginindza, T. G. G. and Giussani, G. and Gnedovskaya, E. V. and Goharinezhad, S. and Gopalani, S. V. and Gorini, G. and Goudarzi, H. and Goulart, A. C. and Greaves, F. and Grivna, M. and Grosso, G. and Gubari, M. I. M. and Gugnani, H. C. and Guimarães, R. A. and Guled, R. A. and Guo, G. and Guo, Y. and Gupta, R. and Gupta, T. and Haddock, B. and Hafezi-Nejad, N. and Hafiz, A. and Haj-Mirzaian, A. and Haj-Mirzaian, A. and Hall, B. J. and Halvaei, I. and Hamadeh, R. R. and Hamidi, S. and Hammer, M. S. and Hankey, G. J. and Haririan, H. and Haro, J. M. and Hasaballah, A. I. and Hasan, M. M. and Hasanpoor, E. and Hashi, A. and Hassanipour, S. and Hassankhani, H. and Havmoeller, R. J. and Hay, S. I. and Hayat, K. and Heidari, G. and Heidari-Soureshjani, R. and Henrikson, H. J. and Herbert, M. E. and Herteliu, C. and Heydarpour, F. and Hird, T. R. and Hoek, H. W. and Holla, R. and Hoogar, P. and Hosgood, H. D. and Hossain, N. and Hosseini, M. and Hosseinzadeh, M. and Hostiuc, M. and Hostiuc, S. and Househ, M. and Hsairi, M. and Hsieh, V. C.-r. and Hu, G. and Hu, K. and Huda, T. M. and Humayun, A. and Huynh, C. K. and Hwang, B.-F. and Iannucci, V. C. and Ibitoye, S. E. and Ikeda, N. and Ikuta, K. S. and Ilesanmi, O. S. and Ilic, I. M. and Ilic, M. D. and Inbaraj, L. R. and Ippolito, H. and Iqbal, U. and Irvani, S. S. N. and Irvine, C. M. S. and Islam, M. M. and Islam, S. M. S. and Iso, H. and Ivers, R. Q. and Iwu, C. C. D. and Iwu, C. J. and Iyamu, I. O. and Jaafari, J. and Jacobsen, K. H. and Jafari, H. and Jafarinia, M. and Jahani, M. A. and Jakovljevic, M. and Jalilian, F. and James, S. L. and Janjani, H. and Javaheri, T. and Javidnia, J. and Jeemon, P. and Jenabi, E. and Jha, R. P. and Jha, V. and Ji, J. S. and Johansson, L. and John, O. and John-Akinola, Y. O. and Johnson, C. O. and Jonas, J. B. and Joukar, F. and Jozwiak, J. J. and Jürisson, M. and Kabir, A. and Kabir, Z. and Kalani, H. and Kalani, R. and Kalankesh, L. R. and Kalhor, R. and Kanchan, T. and Kapoor, N. and Karami Matin, B. and Karch, A. and Karim, M. A. and Kassa, G. M. and Katikireddi, S. V. and Kayode, G. A. and Kazemi Karyani, A. and Keiyoro, P. N. and Keller, C. and Kemmer, L. and Kendrick, P. J. and Khalid, N. and Khammarnia, M. and Khan, E. A. and Khan, M. and Khatab, K. and Khater, M. M. and Khatib, M. N. and Khayamzadeh, M. and Khazaei, S. and Kieling, C. and Kim, Y. J. and Kimokoti, R. W. and Kisa, A. and Kisa, S. and Kivimäki, M. and Knibbs, L. D. and Knudsen, A. K. S. and Kocarnik, J. M. and Kochhar, S. and Kopec, J. A. and Korshunov, V. A. and Koul, P. A. and Koyanagi, A. and Kraemer, M. U. G. and Krishan, K. and Krohn, K. J. and Kromhout, H. and Kuate Defo, B. and Kumar, G. A. and Kumar, V. and Kurmi, O. P. and Kusuma, D. and La Vecchia, C. and Lacey, B. and Lal, D. K. and Lalloo, R. and Lallukka, T. and Lami, F. H. and Landires, I. and Lang, J. J. and Langan, S. M. and Larsson, A. O. and Lasrado, S. and Lauriola, P. and Lazarus, J. V. and Lee, P. H. and Lee, S. W. H. and LeGrand, K. E. and Leigh, J. and Leonardi, M. and Lescinsky, H. and

Leung, J. and Levi, M. and Li, S. and Lim, L.-L. and Linn, S. and Liu, S. and Liu, S. and Liu, Y. and Lo, J. and Lopez, A. D. and Lopez, J. C. F. and Lopukhov, P. D. and Lorkowski, S. and Lotufo, P. A. and Lu, A. and Lugo, A. and Maddison, E. R. and Mahasha, P. W. and Mahdavi, M. M. and Mahmoudi, M. and Majeed, A. and Maleki, A. and Maleki, S. and Malekzadeh, R. and Malta, D. C. and Mamun, A. A. and Manda, A. L. and Manguerra, H. and Mansour-Ghanaei, F. and Mansouri, B. and Mansournia, M. A. and Mantilla Herrera, A. M. and Maravilla, J. C. and Marks, A. and Martin, R. V. and Martini, S. and Martins-Melo, F. R. and Masaka, A. and Masoumi, S. Z. and Mathur, M. R. and Matsushita, K. and Maulik, P. K. and McAlinden, C. and McGrath, J. J. and McKee, M. and Mehndiratta, M. M. and Mehri, F. and Mehta, K. M. and Memish, Z. A. and Mendoza, W. and Menezes, R. G. and Mengesha, E. W. and Mereke, A. and Mereta, S. T. and Meretoja, A. and Meretoja, T. J. and Mestrovic, T. and Miazgowski, B. and Miazgowski, T. and Michalek, I. M. and Miller, T. R. and Mills, E. J. and Mini, G. K. and Miri, M. and Mirica, A. and Mirrakhimov, E. M. and Mirzaei, H. and Mirzaei, M. and Mirzaei, R. and Mirzaei-Alavijeh, M. and Misganaw, A. T. and Mithra, P. and Moazen, B. and Mohammad, D. K. and Mohammad, Y. and Mohammad Gholi Mezerji, N. and Mohammadian-Hafshejani, A. and Mohammadifard, N. and Mohammadpourhodki, R. and Mohammed, A. S. and Mohammed, H. and Mohammed, J. A. and Mohammed, S. and Mokdad, A. H. and Molokhia, M. and Monasta, L. and Mooney, M. D. and Moradi, G. and Moradi, M. and Moradi-Lakeh, M. and Moradzadeh, R. and Moraga, P. and Morawska, L. and Morgado-da-Costa, J. and Morrison, S. D. and Mosapour, A. and Mosser, J. F. and Mouodi, S. and Mousavi, S. M. and Mousavi Khaneghah, A. and Mueller, U. O. and Mukhopadhyay, S. and Mullany, E. C. and Musa, K. I. and Muthupandian, S. and Nabhan, A. F. and Naderi, M. and Nagarajan, A. J. and Nagel, G. and Naghavi, M. and Naghshtabrizi, B. and Naimzada, M. D. and Najafi, F. and Nangia, V. and Nansseu, J. R. and Naserbakht, M. and Nayak, V. C. and Negoi, I. and Ngunjiri, J. W. and Nguyen, C. T. and Nguyen, H. L. T. and Nguyen, M. and Nigatu, Y. T. and Nikbakhsh, R. and Nixon, M. R. and Nnaji, C. A. and Nomura, S. and Norrving, B. and Noubiap, J. J. and Nowak, C. and Nunez-Samudio, V. and Oţoiu, A. and Oancea, B. and Odell, C. M. and Ogbo, F. A. and Oh, I.-H. and Okunga, E. W. and Oladnabi, M. and Olagunju, A. T. and Olusanya, B. O. and Olusanya, J. O. and Omer, M. O. and Ong, K. L. and Onwujekwe, O. E. and Orpana, H. M. and Ortiz, A. and Osarenotor, O. and Osei, F. B. and Ostroff, S. M. and Otstavnov, N. and Otstavnov, S. S. and Øverland, S. and Owolabi, M. O. and P A, M. and Padubidri, J. R. and Palladino, R. and Panda-Jonas, S. and Pandey, A. and Parry, C. D. H. and Pasovic, M. and Pasupula, D. K. and Patel, S. K. and Pathak, M. and Patten, S. B. and Patton, G. C. and Pazoki Toroudi, H. and Peden, A. E. and Pennini, A. and Pepito, V. C. F. and Peprah, E. K. and Pereira, D. M. and Pesudovs, K. and Pham, H. Q. and Phillips, M. R. and Piccinelli, C. and Pilz, T. M. and Piradov, M. A. and Pirsaheb, M. and Plass, D. and Polinder, S. and Polkinghorne, K. R. and Pond, C. D. and Postma, M. J. and Pourjafar, H. and Pourmalek, F. and Poznańska, A. and Prada, S. I. and Prakash, V. and Pribadi, D. R. A. and Pupillo, E. and Quazi Syed, Z. and Rabiee, M. and Rabiee, N. and Radfar, A. and Rafiee, A. and Raggi, A. and Rahman, M. A. and Rajabpour-Sanati, A. and Rajati, F. and Rakovac, I. and Ram, P. and Ramezanzadeh, K. and Ranabhat, C. L. and Rao, P. C. and Rao, S. J. and Rashedi, V. and Rathi, P. and Rawaf, D. L. and Rawaf, S. and Rawal, L. and Rawassizadeh, R. and Rawat, R. and Razo, C. and Redford, S. B. and Reiner, R. C., Jr.

and Reitsma, M. B. and Remuzzi, G. and Renjith, V. and Renzaho, A. M. N. and Resnikoff, S. and Rezaei, N. and Rezaei, N. and Rezapour, A. and Rhinehart, P.-A. and Riahi, S. M. and Ribeiro, D. C. and Ribeiro, D. and Rickard, J. and Rivera, J. A. and Roberts, N. L. S. and Rodríguez-Ramírez, S. and Roever, L. and Ronfani, L. and Room, R. and Roshandel, G. and Roth, G. A. and Rothenbacher, D. and Rubagotti, E. and Rwegerera, G. M. and Sabour, S. and Sachdev, P. S. and Saddik, B. and Sadeghi, E. and Sadeghi, M. and Saeedi, R. and Saeedi Moghaddam, S. and Safari, Y. and Safi, S. and Safiri, S. and Sagar, R. and Sahebkar, A. and Sajadi, S. M. and Salam, N. and Salamati, P. and Salem, H. and Salem, M. R. R. and Salimzadeh, H. and Salman, O. M. and Salomon, J. A. and Samad, Z. and Samadi Kafil, H. and Sambala, E. Z. and Samy, A. M. and Sanabria, J. and Sánchez-Pimienta, T. G. and Santomauro, D. F. and Santos, I. S. and Santos, J. V. and Santric-Milicevic, M. M. and Saraswathy, S. Y. I. and Sarmiento-Suárez, R. and Sarrafzadegan, N. and Sartorius, B. and Sarveazad, A. and Sathian, B. and Sathish, T. and Sattin, D. and Saxena, S. and Schaeffer, L. E. and Schiavolin, S. and Schlaich, M. P. and Schmidt, M. I. and Schutte, A. E. and Schwebel, D. C. and Schwendicke, F. and Senbeta, A. M. and Senthilkumaran, S. and Sepanlou, S. G. and Serdar, B. and Serre, M. L. and Shadid, J. and Shafaat, O. and Shahabi, S. and Shaheen, A. A. and Shaikh, M. A. and Shalash, A. S. and Shams-Beyranvand, M. and Shamsizadeh, M. and Sharafi, K. and Sheikh, A. and Sheikhtaheri, A. and Shibuya, K. and Shield, K. D. and Shigematsu, M. and Shin, J. I. and Shin, M.-J. and Shiri, R. and Shirkoohi, R. and Shuval, K. and Siabani, S. and Sierpinski, R. and Sigfusdottir, I. D. and Sigurvinsdottir, R. and Silva, J. P. and Simpson, K. E. and Singh, J. A. and Singh, P. and Skiadaresi, E. and Skou, S. T. S. and Skryabin, V. Y. and Smith, E. U. R. and Soheili, A. and Soltani, S. and Soofi, M. and Sorensen, R. J. D. and Soriano, J. B. and Sorrie, M. B. and Soshnikov, S. and Soyiri, I. N. and Spencer, C. N. and Spotin, A. and Sreeramareddy, C. T. and Srinivasan, V. and Stanaway, J. D. and Stein, C. and Stein, D. J. and Steiner, C. and Stockfelt, L. and Stokes, M. A. and Straif, K. and Stubbs, J. L. and Sufiyan, M. a. B. and Suleria, H. A. R. and Suliankatchi Abdulkader, R. and Sulo, G. and Sultan, I. and Szumowski, Ł. and Tabarés-Seisdedos, R. and Tabb, K. M. and Tabuchi, T. and Taherkhani, A. and Tajdini, M. and Takahashi, K. and Takala, J. S. and Tamiru, A. T. and Taveira, N. and Tehrani-Banihashemi, A. and Temsah, M.-H. and Tesema, G. A. and Tessema, Z. T. and Thurston, G. D. and Titova, M. V. and Tohidinik, H. R. and Tonelli, M. and Topor-Madry, R. and Topouzis, F. and Torre, A. E. and Touvier, M. and Tovani-Palone, M. R. R. and Tran, B. X. and Travillian, R. and Tsatsakis, A. and Tudor Car, L. and Tyrovolas, S. and Uddin, R. and Umeokonkwo, C. D. and Unnikrishnan, B. and Upadhyay, E. and Vacante, M. and Valdez, P. R. and van Donkelaar, A. and Vasankari, T. J. and Vasseghian, Y. and Veisani, Y. and Venketasubramanian, N. and Violante, F. S. and Vlassov, V. and Vollset, S. E. and Vos, T. and Vukovic, R. and Waheed, Y. and Wallin, M. T. and Wang, Y. and Wang, Y.-P. and Watson, A. and Wei, J. and Wei, M. Y. W. and Weintraub, R. G. and Weiss, J. and Werdecker, A. and West, J. J. and Westerman, R. and Whisnant, J. L. and Whiteford, H. A. and Wiens, K. E. and Wolfe, C. D. A. and Wozniak, S. S. and Wu, A.-M. and Wu, J. and Wulf Hanson, S. and Xu, G. and Xu, R. and Yadgir, S. and Yahyazadeh Jabbari, S. H. and Yamagishi, K. and Yaminfirooz, M. and Yano, Y. and Yaya, S. and Yazdi-Feyzabadi, V. and Yeheyis, T. Y. and Yilgwan, C. S. and Yilma, M. T. and Yip, P. and Yonemoto, N. and Younis, M. Z. and Younker, T. P. and Yousefi, B. and Yousefi, Z. and Yousefinezhadi, T. and Yousuf,

A. Y. and Yu, C. and Yusefzadeh, H. and Zahirian Moghadam, T. and Zamani, M. and Zamanian, M. and Zandian, H. and Zastrozhin, M. S. and Zhang, Y. and Zhang, Z.-J. and Zhao, J. T. and Zhao, X.-J. G. and Zhao, Y. and Zhou, M. and Ziapour, A. and Zimsen, S. R. M. and Brauer, M. and Afshin, A. and Lim, S. S.: Global burden of 87 risk factors in 204 countries and territories, 1990-2019: a systematic analysis for the Global Burden of Disease Study 2019, The Lancet, 396, 1223-1249, 10.1016/S0140-6736(20)30752-2, 2020.

New York City Department of Health and Mental Hygiene. EpiQuery - [Syndromic Surveillance Data 2023]. [accessed on September 26: [dataset], 2023.

Ng, N. L., Canagaratna, M. R., Jimenez, J. L., Chhabra, P. S., Seinfeld, J. H., and Worsnop, D. R.: Changes in organic aerosol composition with aging inferred from aerosol mass spectra, Atmos. Chem. Phys., 11, 6465-6474, 10.5194/acp-11-6465-2011, 2011a.

Ng, N. L., Herndon, S. C., Trimborn, A., Canagaratna, M. R., Croteau, P. L., Onasch, T. B., Sueper, D., Worsnop, D. R., Zhang, Q., Sun, Y. L., and Jayne, J. T.: An Aerosol Chemical Speciation Monitor (ACSM) for Routine Monitoring of the Composition and Mass Concentrations of Ambient Aerosol, Aerosol Science and Technology, 45, 780-794, 10.1080/02786826.2011.560211, 2011b.

Ng, N. L., Canagaratna, M. R., Zhang, Q., Jimenez, J. L., Tian, J., Ulbrich, I. M., Kroll, J. H., Docherty, K. S., Chhabra, P. S., Bahreini, R., Murphy, S. M., Seinfeld, J. H., Hildebrandt, L., Donahue, N. M., DeCarlo, P. F., Lanz, V. A., Prévôt, A. S. H., Dinar, E., Rudich, Y., and Worsnop, D. R.: Organic aerosol components observed in Northern Hemispheric datasets from Aerosol Mass Spectrometry, Atmos. Chem. Phys., 10, 4625-4641, 10.5194/acp-10-4625-2010, 2010.

O'Dell, K., Bilsback, K., Ford, B., Martenies, S. E., Magzamen, S., Fischer, E. V., and Pierce, J. R.: Estimated Mortality and Morbidity Attributable to Smoke Plumes in the United States: Not Just a Western US Problem, GeoHealth, 5, e2021GH000457, https://doi.org/10.1029/2021GH000457, 2021.

Pachon, J. E., Weber, R. J., Zhang, X., Mulholland, J. A., and Russell, A. G.: Revising the use of potassium (K) in the source apportionment of PM2.5, Atmospheric Pollution Research, 4, 14-21, 10.5094/apr.2013.002, 2013.

Palm, B. B., Peng, Q., Fredrickson, C. D., Lee, B. H., Garofalo, L. A., Pothier, M. A., Kreidenweis, S. M., Farmer, D. K., Pokhrel, R. P., Shen, Y., Murphy, S. M., Permar, W., Hu, L., Campos, T. L., Hall, S. R., Ullmann, K., Zhang, X., Flocke, F., Fischer, E. V., and Thornton, J. A.: Quantification of organic aerosol and brown carbon evolution in fresh wildfire plumes, Proceedings of the National Academy of Sciences, 202012218, 10.1073/pnas.2012218117, 2020.

Parrish, D. D., Singh, H. B., Molina, L., and Madronich, S.: Air quality progress in North American megacities: A review, Atmospheric Environment, 45, 7015-7025, https://doi.org/10.1016/j.atmosenv.2011.09.039, 2011.

Pebesma, E. and Bivand, R.: Spatial data science: With applications in R, CRC Press2023.

Permar, W., Wang, Q., Selimovic, V., Wielgasz, C., Yokelson, R. J., Hornbrook, R. S., Hills, A. J., Apel, E. C., Ku, I. T., Zhou, Y., Sive, B. C., Sullivan, A. P., Collett Jr, J. L., Campos, T. L., Palm, B. B., Peng, Q., Thornton, J. A., Garofalo, L. A., Farmer, D. K., Kreidenweis, S. M., Levin, E. J. T., DeMott, P. J., Flocke, F., Fischer, E. V., and Hu, L.: Emissions of Trace Organic Gases From Western U.S. Wildfires Based on WE-CAN

Aircraft Measurements, Journal of Geophysical Research: Atmospheres, 126, e2020JD033838, https://doi.org/10.1029/2020JD033838, 2021.
Pye, H. O. T., Ward-Caviness, C. K., Murphy, B. N., Appel, K. W., and Seltzer, K. M.: Secondary organic aerosol association with cardiorespiratory disease mortality in the United States, Nature Communications, 12, 7215, 10.1038/s41467-021-27484-1, 2021.
Reid, J. S., Koppmann, R., Eck, T. F., and Eleuterio, D. P.: A review of biomass burning emissions part II: intensive physical properties of biomass burning particles, Atmos. Chem. Phys., 5, 799-825, 10.5194/acp-5-799-2005, 2005.
Rogers, H. M., Ditto, J. C., and Gentner, D. R.: Evidence for impacts on surface-level air quality in the northeastern US from long-distance transport of smoke from North American fires during the Long Island Sound Tropospheric Ozone Study (LISTOS) 2018, Atmos. Chem. Phys., 20, 671-682, 10.5194/acp-20-671-2020, 2020.
Sekimoto, K., Koss, A. R., Gilman, J. B., Selimovic, V., Coggon, M. M., Zarzana, K. J., Yuan, B., Lerner, B. M., Brown, S. S., Warneke, C., Yokelson, R. J., Roberts, J. M., and de Gouw, J.: High- and low-temperature pyrolysis profiles describe volatile organic compound emissions from western US wildfire fuels, Atmospheric Chemistry and Physics, 18, 9263-9281, 10.5194/acp-18-9263-2018, 2018.
Stein, A. F., Draxler, R. R., Rolph, G. D., Stunder, B. J. B., Cohen, M. D., and Ngan, F.: NOAA's HYSPLIT Atmospheric Transport and Dispersion Modeling System, Bulletin of the American Meteorological Society, 96, 2059-2077, https://doi.org/10.1175/BAMS-D-14-00110.1, 2015.
Sullivan, A. P., Holden, A. S., Patterson, L. A., McMeeking, G. R., Kreidenweis, S. M., Malm, W. C., Hao, W. M., Wold, C. E., and Collett, J. L.: A method for smoke marker measurements and its potential application for determining the contribution of biomass burning from wildfires and prescribed fires to ambient PM2.5 organic carbon, Journal of Geophysical Research: Atmospheres, 113, 10.1029/2008jd010216, 2008.
Thorpe, A. and Harrison, R. M.: Sources and properties of non-exhaust particulate matter from road traffic: A review, Science of The Total Environment, 400, 270-282, https://doi.org/10.1016/j.scitotenv.2008.06.007, 2008.
Thurston, G., Yu, W., and Luglio, D.: An Evaluation of the Asthma Impact of the June 2023 New York City Wildfire Air Pollution Episode, American Journal of Respiratory and Critical Care Medicine, 208, 898-900, 10.1164/rccm.202306-1073LE, 2023.
Tuet, W. Y., Chen, Y., Fok, S., Champion, J. A., and Ng, N. L.: Inflammatory responses to secondary organic aerosols (SOA) generated from biogenic and anthropogenic precursors, Atmos. Chem. Phys., 17, 11423-11440, 10.5194/acp-17-11423-2017, 2017.
Val Martin, M., Logan, J. A., Kahn, R. A., Leung, F. Y., Nelson, D. L., and Diner, D. J.: Smoke injection heights from fires in North America: analysis of 5 years of satellite observations, Atmos. Chem. Phys., 10, 1491-1510, 10.5194/acp-10-1491-2010, 2010.
Vasilakopoulou, C. N., Matrali, A., Skyllakou, K., Georgopoulou, M., Aktypis, A., Florou, K., Kaltsonoudis, C., Siouti, E., Kostenidou, E., Błaziak, A., Nenes, A., Papagiannis, S., Eleftheriadis, K., Patoulias, D., Kioutsioukis, I., and Pandis, S. N.: Rapid transformation of wildfire emissions to harmful background aerosol, npj Climate and Atmospheric Science, 6, 218, 10.1038/s41612-023-00544-7, 2023.
Verma, V., Fang, T., Xu, L., Peltier, R. E., Russell, A. G., Ng, N. L., and Weber, R. J.: Organic Aerosols Associated with the Generation of Reactive Oxygen Species (ROS) by Water-

Soluble PM2.5, Environmental Science & Technology, 49, 4646-4656, 10.1021/es505577w, 2015.

Weichenthal, S., Pinault, L., Christidis, T., Burnett, R. T., Brook, J. R., Chu, Y., Crouse, D. L., Erickson, A. C., Hystad, P., Li, C., Martin, R. V., Meng, J., Pappin, A. J., Tjepkema, M., van Donkelaar, A., Weagle, C. L., and Brauer, M.: How low can you go? Air pollution affects mortality at very low levels, Science Advances, 8, eabo3381, doi:10.1126/sciadv.abo3381, 2022.

Wu, Y., Arapi, A., Huang, J., Gross, B., and Moshary, F.: Intra-continental wildfire smoke transport and impact on local air quality observed by ground-based and satellite remote sensing in New York City, Atmospheric Environment, 187, 266-281, https://doi.org/10.1016/j.atmosenv.2018.06.006, 2018.

Xu, L., Crounse John, D., Vasquez Krystal, T., Allen, H., Wennberg Paul, O., Bourgeois, I., Brown Steven, S., Campuzano-Jost, P., Coggon Matthew, M., Crawford James, H., DiGangi Joshua, P., Diskin Glenn, S., Fried, A., Gargulinski Emily, M., Gilman Jessica, B., Gkatzelis Georgios, I., Guo, H., Hair Johnathan, W., Hall Samuel, R., Halliday Hannah, A., Hanisco Thomas, F., Hannun Reem, A., Holmes Christopher, D., Huey, L. G., Jimenez Jose, L., Lamplugh, A., Lee Young, R., Liao, J., Lindaas, J., Neuman, J. A., Nowak John, B., Peischl, J., Peterson David, A., Piel, F., Richter, D., Rickly Pamela, S., Robinson Michael, A., Rollins Andrew, W., Ryerson Thomas, B., Sekimoto, K., Selimovic, V., Shingler, T., Soja Amber, J., St. Clair Jason, M., Tanner David, J., Ullmann, K., Veres Patrick, R., Walega, J., Warneke, C., Washenfelder Rebecca, A., Weibring, P., Wisthaler, A., Wolfe Glenn, M., Womack Caroline, C., and Yokelson Robert, J.: Ozone chemistry in western U.S. wildfire plumes, Science Advances, 7, eabl3648, 10.1126/sciadv.abl3648, 2022.

Yu, J., Yan, C., Liu, Y., Li, X., Zhou, T., and Zheng, M.: Potassium: A Tracer for Biomass Burning in Beijing?, Aerosol and Air Quality Research, 18, 2447-2459, 10.4209/aaqr.2017.11.0536, 2018.

Yu, Q., Chen, J., Qin, W., Ahmad, M., Zhang, Y., Sun, Y., Xin, K., and Ai, J.: Oxidative potential associated with water-soluble components of PM2.5 in Beijing: The important role of anthropogenic organic aerosols, Journal of Hazardous Materials, 433, 128839, https://doi.org/10.1016/j.jhazmat.2022.128839, 2022.

Zeger, S. L., Irizarry, R., and Peng, R. D.: On Time Series Analysis of Public Health and Biomedical Data, Annual Review of Public Health, 27, 57-79, 10.1146/annurev.publhealth.26.021304.144517, 2006.

Zhang, Q., Jimenez, J. L., Canagaratna, M. R., Ulbrich, I. M., Ng, N. L., Worsnop, D. R., and Sun, Y.: Understanding atmospheric organic aerosols via factor analysis of aerosol mass spectrometry: a review, Analytical and Bioanalytical Chemistry, 401, 3045-3067, 10.1007/s00216-011-5355-y, 2011.

Zhou, J., Elser, M., Huang, R. J., Krapf, M., Fröhlich, R., Bhattu, D., Stefenelli, G., Zotter, P., Bruns, E. A., Pieber, S. M., Ni, H., Wang, Q., Wang, Y., Zhou, Y., Chen, C., Xiao, M., Slowik, J. G., Brown, S., Cassagnes, L. E., Daellenbach, K. R., Nussbaumer, T., Geiser, M., Prévôt, A. S. H., El-Haddad, I., Cao, J., Baltensperger, U., and Dommen, J.: Predominance of secondary organic aerosol to particle-bound reactive oxygen species activity in fine ambient aerosol, Atmos. Chem. Phys., 19, 14703-14720, 10.5194/acp-19-14703-2019, 2019.

Acknowledgements

We thank the New York State Department of Environmental Conservation for site access, support, and supporting data, including gaseous formaldehyde. The meteorology data from the Queens College site was made possible by the New York State (NYS) Mesonet.

Funding: This research was supported by National Science Foundation (AGS-2131914) and New York State Research and Development Authority (NYSERDA; Agreement No. 183866). NYS Mesonet was originally supported by Federal Emergency Management Agency Grant FEMA-4085-DR-NY, with the continued support of the NYS Division of Homeland Security and Emergency Services; the State of New York; the Research Foundation for the State University of New York (SUNY); the University at Albany; the Atmospheric Sciences Research Center (ASRC) at the University at Albany; and the Department of Atmospheric and Environmental Sciences (DAES) at the University at Albany.

Note: Any opinions expressed in this article do not necessarily reflect those of NYSERDA or the State of New York.

Author contributions: T.J. and D.R.G. conceptualized and designed the study, T.J., M.J.R., and T.H-M. collected data, T.J., M.J.R., C.S., and T.H-M. analyzed and visualized data with N.L.N.'s and D.R.G.'s guidance. S.H. and M.B. performed the epidemiological analysis. T.J., M.J.R., and D.R.G. wrote the original manuscript. All authors reviewed and edited the manuscript.

Competing interests: Authors declare no competing interests.

Data and materials availability: Data will be made publicly available via the ASCENT data repository.

Figures and Tables

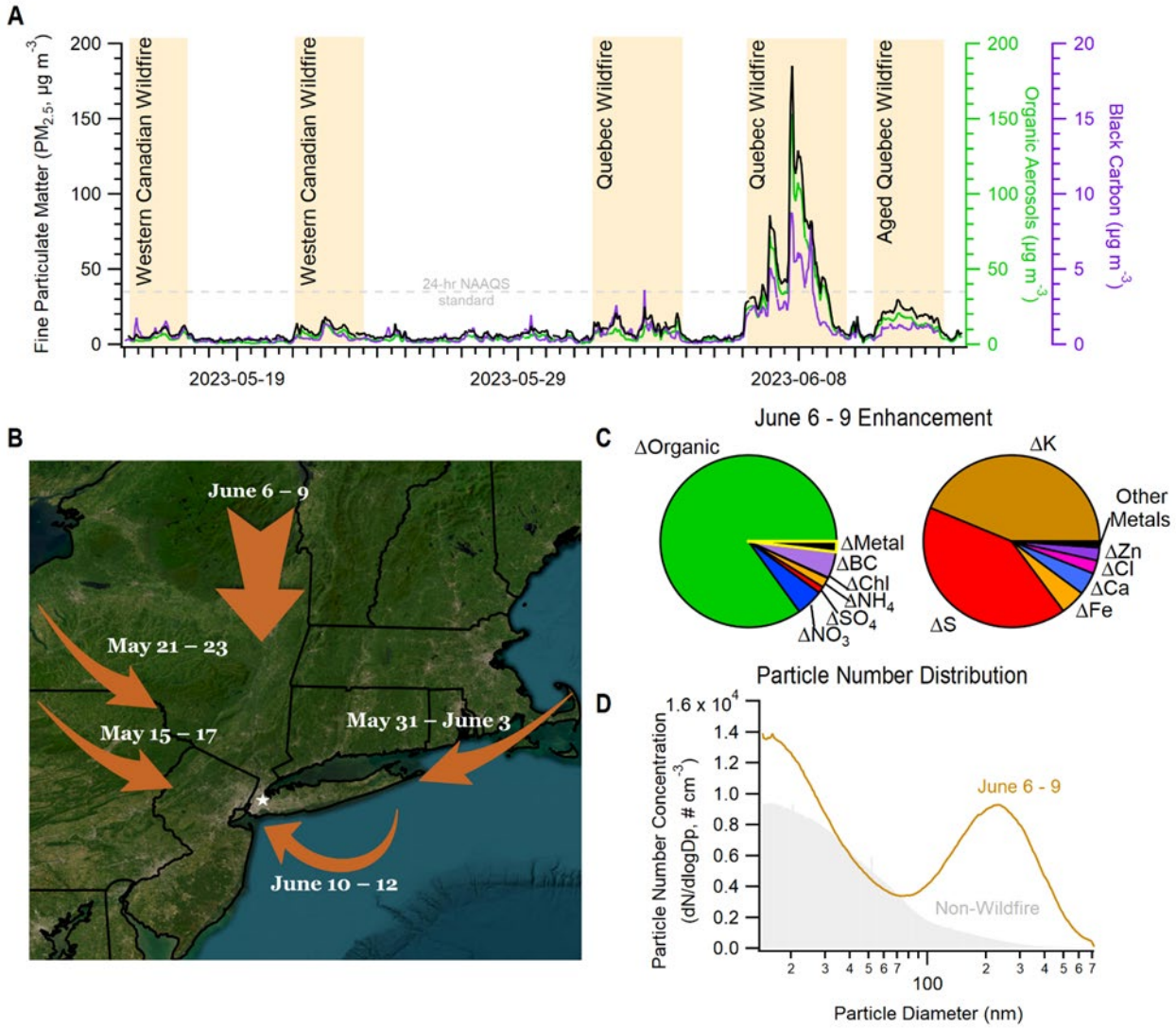

Fig. 1. Air quality impacts from smoke transport to New York City. (A) Hourly fine particulate matter ($PM_{2.5}$) concentrations (i.e., sum of organic, inorganic, black carbon, and trace metals), with organic aerosols and black carbon concentrations shown across five major smoke transport events, including the June 6-9, 2023 transport of Quebec wildfire smoke. **(B)** Summary of plumes from May 15 to June 13, 2023, with more detailed descriptions of each episode's origin, arrival, and wind roses in Fig. S2 and S3. **(C)** June 6-9, 2023 enhancements of organic and inorganic (i.e., nitrate (NO_3), sulfate (SO_4), ammonium (NH_4), black carbon) particulate matter components and associated trace metals, relative to non-fire influenced periods (Note: total mass fraction in yellow wedge of left pie chart is speciated in the right pie chart). **(D)** Submicron size distributions of particle number concentrations during June 6-9, 2023, compared to non-wildfire periods.

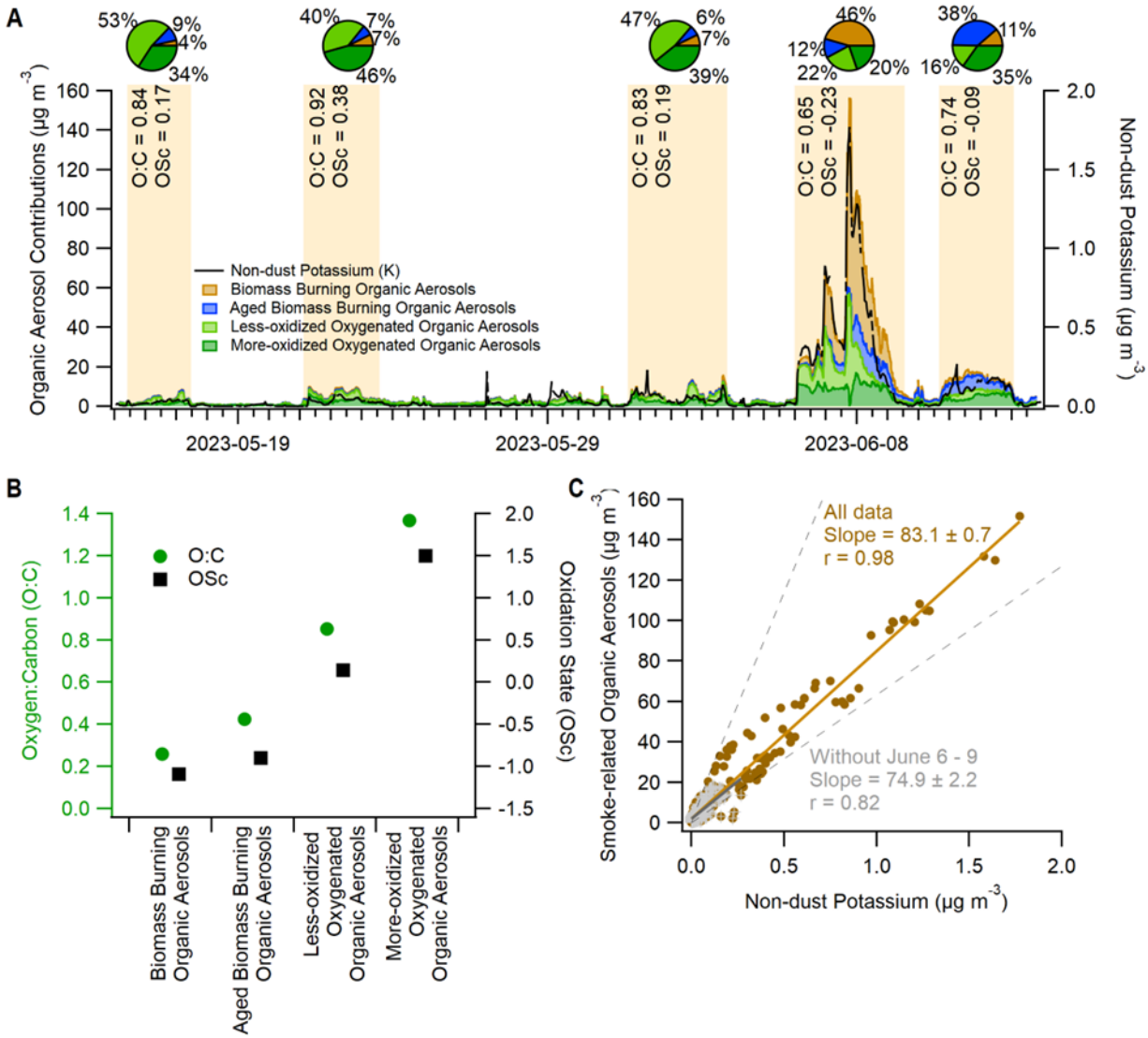

Fig. 2. Transported smoke observed predominantly as generic aged organic aerosols with the fraction of evident biomass burning-related organic aerosols varying between fire events. (A) The influence of transported smoke detected across different aerosol types (i.e., factors) observed as both directly-emitted biomass burning organic aerosols and oxidized organic aerosol types with **(B)** increasing average oxygen-to-carbon ratios (O:C) and oxidation states (OSc), which together capture the contributions of organic aerosols from transported smoke during the study period. **(C)** The sum of smoke-related enhancements in these four organic aerosol types were best correlated with non-dust potassium, during June 6-9, 2023 and the other smoke events. Black dashed lines signify the 2σ range of μg μgK^{-1} ratios during all wildfire smoke transport episodes. Contributions of cooking- and hydrocarbon-related organic aerosols can be found in Fig. S5.

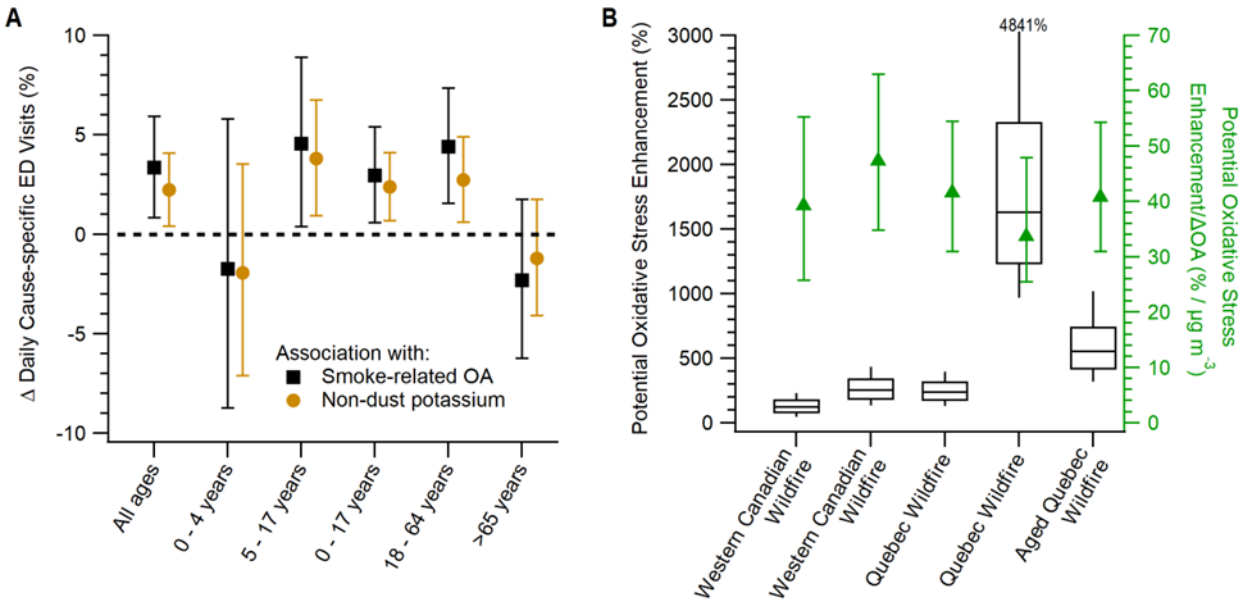

Fig. 3. Observed health effects associated with smoke transport and potential oxidative stress enhancements across study period. (A) Observed association between asthma emergency department (ED) visits and smoke-related organic aerosols (i.e., sum of 4 factors) as well as non-dust potassium as a confirmational marker of both "fresh" and aged smoke. Epidemiological results shown as the % change in ED visits for an interquartile range increase in concentrations with vertical lines displaying 95% confidence intervals. **(B)** Estimates of potential oxidative stress enhancements (left axis) for each of the 5 smoke transport events compared to background conditions, determined via Monte Carlo analysis ($N=1\times10^6$) using available studies. Shown alongside the concentration-normalized potential oxidative stress enhancement (right axis) with more-aged smoke showing greater potential oxidative stress per organic aerosol mass, on average, for the episodes outside of June 6-9.